AEDC-TR-94-3

Optical Analysis Methods for Material Films Condensed on Cryogenic Surfaces of Spacecraft

K. F. Palmer, M. Z. Williams, and B. A. Budde
Westminster College
Fulton, MO

W. T. Bertrand
Calspan Corporation/AEDC Operations

August 1994

Final Report for Period March 1993 – September 1993

Approved for public release; distribution is unlimited.

ARNOLD ENGINEERING DEVELOPMENT CENTER
ARNOLD AIR FORCE BASE, TENNESSEE
AIR FORCE MATERIEL COMMAND
UNITED STATES AIR FORCE

NOTICES

When U. S. Government drawings, specifications, or other data are used for any purpose other than a definitely related Government procurement operation, the Government thereby incurs no responsibility nor any obligation whatsoever, and the fact that the Government may have formulated, furnished, or in any way supplied the said drawings, specifications, or other data, is not to be regarded by implication or otherwise, or in any manner licensing the holder or any other person or corporation, or conveying any rights or permission to manufacture, use, or sell any patented invention that may in any way be related thereto.

Qualified users may obtain copies of this report from the Defense Technical Information Center.

References to named commercial products in this report are not to be considered in any sense as an endorsement of the product by the United States Air Force or the Government.

This report has been reviewed by the Office of Public Affairs (PA) and is releasable to the National Technical Information Service (NTIS). At NTIS, it will be available to the general public, including foreign nations.

APPROVAL STATEMENT

This report has been reviewed and approved:

Jerry F Fairchild

JERRY F. FAIRCHILD, Captain, USAF
Applied Technology Division

Approved for Publication:

FOR THE COMMANDER

Robert T. Crook

ROBERT T. CROOK
Assistant Chief, Applied Technology Division

REPORT DOCUMENTATION PAGE

Form Approved
OMB No. 0704-0188

Public reporting burden for this collection of information is estimated to average 1 hour per response, including the time for reviewing instructions, searching existing data sources, gathering and maintaining the data needed, and completing and reviewing the collection of information. Send comments regarding this burden estimate or any other aspect of this collection of information, including suggestions for reducing this burden, to Washington Headquarters Services, Directorate for Information Operations and Reports, 1215 Jefferson Davis Highway, Suite 1204, Arlington, VA 22202-4302, and to the Office of Management and Budget, Paperwork Reduction Project (0704-0188), Washington, DC 20503

1. AGENCY USE ONLY (Leave blank)	2. REPORT DATE	3. REPORT TYPE AND DATES COVERED
	August 1994	Final Report for Mar. 1993 - Sept. 1993

4. TITLE AND SUBTITLE

Optical Analysis Methods for Material Films Condensed on Cryogenic Surfaces of Spacecraft

5. FUNDING NUMBERS

-0107

6. AUTHOR(S)

K.F. Palmer, M. Z. Williams, and B.A. Budde, Westminister College; W.T. Bertrand, Calspan Corporation/AEDC Operations

7. PERFORMING ORGANIZATION NAME(S) AND ADDRESS(ES)

Arnold Engineering Development Center/DOT
Air Force Materiel Command
Arnold Air Foce Base, TN 37389-9011

8. PERFORMING ORGANIZATION (REPORT NUMBER)

AEDC-TR-94-4

9. SPONSORING/MONITORING AGENCY NAMES(S) AND ADDRESS(ES)

Arnold Engineering Development Center/DOT
Air Force Materiel Command
Arnold Air Force Base, TN 37389-9011

10. SPONSORING/MONITORING AGENCY REPORT NUMBER

11. SUPPLEMENTARY NOTES

Available in Defense Technical Information Center (DTIC).

12a. DISTRIBUTION/AVAILABILITY STATEMENT

Approved for public release; distribution is unlimited.

12b. DISTRIBUTION CODE

13. ABSTRACT (Maximum 200 words)

Exhaust gases from rocket motors and outgassing products of spacecraft materials can migrate, in a space environment, to other surfaces of the spacecraft and affect their functions. Cryogenically cooled optical systems are particularly vulnerable to these contaminants as are thermal control surfaces and solar cells. One of the goals of the contamination program at AEDC is to predict the optical effects of contaminant layers on optical systems from laboratory measurements of the optical indices, n and k, of contaminant materials. Because the cloud of contaminant molecules, which eventually form a condensate, contain a mixture of molecular species, researchers are seeking ways to predict the optical properties of films composed of constituents using the known properties of each consituent. In this report, the authors examine the physics which describes the optical properties of thin films composed of mixtures of constituents. Examples of the anlysis methods are presented for thin films composed of mixtures using AEDC data on 20K thin films of simple molecules and 80K films condensed from the outgassing products of selected spacecraft materials.

14. SUBJECT TERMS

spacecraft contamination, optical property analysis, contaminant mixtures

15. NUMBER OF PAGES **52**

16. PRICE CODE

17. SECURITY CLASSIFICATION OF REPORT	18. SECURITY CLASSIFICATION OF THIS PAGE	19. SECURITY CLASSIFICATION OF ABSTRACT	20. LIMITATION OF ABSTRACT
UNCLASSIFIED	UNCLASSIFIED	UNCLASSIFIED	SAME AS REPORT

PREFACE

The work reported herein was performed by the Arnold Engineering Development Center (AEDC), Air Force Materiel Command (AFMC) under program element 65807F. The results were obtained by Calspan Corporation, AEDC/Operations, support contractor for aerodynamic testing at the AEDC, AFMC, Arnold Engineering Development Center, Arnold Air Force Base, TN 37389-4300, under AEDC Project No. 0107. The AEDC Project Managers were Maj. M. Maclin and Maj. Mark Briski. The manuscript was submitted for publication on July 6, 1994.

CONTENTS

ILLUSTRATIONS

TABLE

APPENDICES

1.0 INTRODUCTION

Exhaust gases from rocket motors and outgassing products of spacecraft materials can migrate, in a space environment, to other surfaces of the spacecraft and affect their functions (Ref. 1). Cryogenically cooled optical systems are particularly vulnerable to these contaminants as are thermal control surfaces and solar cells.

Recent AEDC research has concentrated on the degradation of optical surfaces by condensed outgassing products of spacecraft materials (Refs. 2, 3, and 4). A prominent feature in the thin-film infrared transmittance spectra of many of these contaminants is a strong absorption band centered at about 3300 cm^{-1} (Ref. 4). Other deleterious absorptions frequently occur at wave number values around 1000 cm^{-1} and less.

One of the goals of the contamination program at AEDC is to predict the optical effects of contaminant layers on optical systems from laboratory measurements of the optical indices, n and k, of contaminant materials. Because the cloud of contaminant molecules, which eventually form a condensate, contains a mixture of molecular species, researchers are seeking ways to predict the optical properties of films composed of constituents using the known properties of each constituent.

In this report, the authors examine the physics which describes the optical properties of thin films composed of mixtures of constituents. We make use of the Lorentz-Lorenz relationship between the optical indices of a material and its polarizability to obtain the optical constants of a mixture of materials. This description is complicated by a lack of detailed knowledge of the intermolecular interactions for the molecules in a given constituent and in a mixture of constituents. An outstanding problem, for example, is to predict accurately the degree of hydrogen-bonding present in any material (Ref. 5).

It is also possible that, because different materials have different outgassing rates, the contaminant layer is, actually, a "stack" of several thin films, each of which has a different composition. Interference effects within each film may or may not be present.

The authors present several examples of the analysis methods for thin films composed of mixtures using AEDC data on 20K thin films of simple molecules and more recent AEDC data of 80K films condensed from the outgassing products of selected spacecraft materials.

2.0 LORENTZ-LORENZ ANALYSIS METHODS

2.1 THE LORENTZ-LORENZ RELATION

The Lorentz-Lorenz relation connects the complex optical index ($\mathbf{n} = n + ik$) of a material with the number density (N) of its constituent molecules, its mean polarizability per molecule (α), and a parameter, b, which relates the "local" electric field, $\vec{E}_{loc}$, actually "felt" by a molecule, with the electric field measured in a cavity of the material, $\vec{E}$. For a linear, isotropic, homogeneous (lih) dielectric material, the classical Lorentz-Lorenz relation is:

$$Na\alpha = (\mathbf{n}^2 - 1) / (\mathbf{n}^2 + b), \tag{1}$$

where

$$b = (\varepsilon_0 a)^{-1} - 1. \tag{2}$$

The constant ε_0 is the electric permittivity of free space, a is another "local" field parameter defined by

$$\vec{E}_{loc} = \vec{E} + a\vec{P}, \tag{3}$$

and $\vec{P}$ is the polarization density vector of the dielectric. If the lih dielectric contains only nonpolar molecules,

$$a = (3\,\varepsilon_0)^{-1}, \text{ and } b = 2. \tag{4}$$

(See Appendix A for a cursory derivation of the Lorentz-Lorenz relation.)

2.2 CALCULATION OF OPTICAL CONSTANTS FOR THE SAME MATERIAL AT DIFFERENT DENSITIES

One can use the relation in any of several ways. For instance, for a single material the Lorentz-Lorenz relation between its optical index and its (mass) density, $\rho = mN$, where m is the (average) mass of a molecule, is,

$$\rho^{-1} (\mathbf{n}^2 - 1) / (\mathbf{n}^2 + b) = a\alpha/m, \text{ a constant.} \tag{5}$$

This constant value (for a given material) is often dubbed the "Lorentz-Lorenz constant" and provides a way to calculate the optical constants of a material at a density value different from the one at which they were originally measured.

2.3 CALCULATION OF THE OPTICAL CONSTANTS OF A MIXTURE

One can also use the Lorentz-Lorenz relation to calculate the optical constants of a mixture of dielectric materials from the optical constants measured for pure samples of each constituent material. The key property of the Lorentz-Lorenz relation that makes this possible is that the index, n_j, measured for a pure sample of the jth constituent material, is related to the (average) polarizability of the molecules contained in the pure jth material as follows:

$$\alpha_j = (N_{pj} a_j)^{-1} \left(n_j^2 - 1\right) / \left(n_j^2 + b_j\right), \tag{6}$$

where N_{pj} is the number density of the jth constituent in the pure sample, and a_j and b_j are the appropriate local field parameters for the pure sample. Furthermore, the (average) molecular polarizability of the mixture, α, is the weighted mean of the polarizabilities of each constituent of the mixture, α_j; that is:

$$\alpha = \Sigma N_j \alpha_j / N \tag{7}$$

where N_j is the number density of the jth constituent in the mixture, and N is the total number density of the molecules in the mixture ($N = \Sigma N_j$). When Eqs. (1), (6), and (7) are combined, the complex index of the mixture turns out to be

$$n = [(1 + bA)/(1 - A)]^{\frac{1}{2}}, \tag{8}$$

and A is a complex number related to the average molecular mass of the mixture ($m = \Sigma N_j m_j / N$), its local field parameters (a and b), its density (ρ), and the densities of the pure materials (ρ_{pj}).

$$A = [(\rho / 1 + b)] \; \Sigma \; [m_j / m (1 + b_j) / \rho_{pj}] \left(n_j^2 - 1\right)\left(n_j^2 + b_j\right). \tag{9}$$

(See Appendix A.)

Equations (8) and (9) form the heart of the algorithm of program NMIX which predicts the optical constants of a film material which is a mixture of materials whose optical constants in their pure states are known.

3.0 OPTICAL ANALYSIS METHODS FOR MULTILAYERED DEPOSITS

If the deposit on a surface consists of a "stack" of uniform layers, each of which has a distinct material composition, the analytical model contained in AEDC programs such as TRNLIN and CALCRT needs to be revised to treat the deposit's optical properties. The analytical model of a

multilayered system is often given in terms of matrix mathematics because the effect of each layer is contained in its own associated "transfer" matrix. The optical effect of the stack is found by computing, in the proper order, the product of the matrices for each layer. It is, therefore, relatively easy to add the effects of additional layers to a given stack by multiplying appropriate additional matrices to the matrix of the original stack.

The transfer matrix of a film which allows interference effects (i.e., allows phase coherence of the beam) relates amplitudes of the components of the beam because amplitudes contain phase information. The transfer matrix of film in which phase coherence does not occur relates beam intensity components and is quite different from the matrix of a film in which phase coherence does occur.

The transfer matrix of a film is often given as a product of matrices, one or two of which represent the changes in the beam at its interfaces and the other gives the effects on the beam as it travels through the film.

3.1 OPTICAL MODEL IN THE CASE OF PHASE COHERENCE IN THE FILMS

In the model we present here, based on the article by Potter (Ref. 6) and briefly discussed in Appendix B, the beam angle of incidence can be from 0 to 90 deg. This means that each electromagnetic wave in the beam has an electric field with two components: the electric field component *perpendicular* (TE) to the plane of incidence (defined by the incident beam and the normal to the incident surface) and the component *parallel* (TM) to the plane of incidence. Because any electric field can be considered a vector sum of these two components, we can study the case of a wave with just a perpendicular electric component (the TE mode, or TEM) separately from the case of a wave with just its parallel electric component (TM mode, or TMM).

3.1.1 TE Mode

If we choose a coordinate system where the z axis lies along the normal of the deposit (and substrate) surfaces, the x axis is perpendicular to the plane of incidence, and, thus, the y axis is parallel to the plane of incidence, we can separate the spatial coordinate and time t dependencies of the electric and magnetic vectors of each electromagnetic wave. In the TE (perpendicular) mode, the electric field in a given medium of index n lies along the x axis and has the form of a product of functions of a separate variable,

$$E_x(y, z, t) = U(z)\, X(y, t), \tag{10}$$

where

$$Uz = E_0 \exp[i2\pi\upsilon nz\cos\phi], \qquad (11)$$

and

$$X(y,t) = \exp[i(2\pi\upsilon ny\sin\phi - \omega t)] \qquad (12)$$

for an electric field of amplitude E_0, vacuum wave number υ, angle ϕ from the surface normal, and angular frequency ω. Similar expressions occur for the y and z components of the magnetic field.

3.1.2 TM Mode

In the TM (parallel) mode, the magnetic field is in the x direction and has the form,

$$Hx(y,z,t) = U(z)X(y,t), \qquad (13)$$

where

$$U(z) = H_0 \exp[i2\pi\upsilon nz\cos\phi] \qquad (14)$$

for a magnetic field of amplitude H_0, and X is defined in Eq. (12). In this report we follow the convention that certain quantities, like U, have different definitions in each mode. Analogous to the TE mode equations, there are expressions similar to Eq. (13) for the y and z components of the electric field.

3.1.3 Phase Coherent Transfer Matrix at an Interface of Two Media

Because the electric and magnetic fields of an electromagnetic wave depend on one other via the Maxwell's Equations, we are able to study the propagation of a wave through a multilayered stack (in the z direction) by noting what happens just to the value of U in either mode. Furthermore, we can distinguish the portion of the fields which propagates in the +z direction from that part going in the -z direction.

Suppose that U in the jth medium has, at the surface the beam exits, a component U_j^+ associated with the wave going in the +z direction and a component U_j^-; let U_{0m}^+ and U_{0m}^- represent the corresponding quantities in the mth medium at the surface the beam enters it. At an interface between the jth and mth media (Fig. 1), these quantities are related by a matrix equation,

$$\begin{bmatrix} U_j^+ \\ U_j^- \end{bmatrix} = S_{jm} \begin{bmatrix} U_{0m}^+ \\ U_{0m}^- \end{bmatrix} \qquad (15)$$

where the amplitude transfer matrix S_{jm} is

$$S_{jm} = \frac{1}{t_{jm}} \begin{bmatrix} 1 & r_{jm} \\ r_{jm} & 1 \end{bmatrix}.$$

The Fresnel transmission and reflection coefficients, t_{jm} and r_{jm}, respectively, are given by

$$t_{jm} = 2\xi_j^{-1} / \left(\xi_j^{-1} + \xi_m^{-1}\right) = 1 + r_{jm}. \tag{16}$$

The quantity ξ_j depends on properties of the jth material and on the mode condition of the wave (Appendix B).

3.1.4 Phase Coherent Transfer Matrix Through a Uniform Medium

The transfer matrix L for a beam going through a uniform medium connects the values of both components of U where the beam enters the medium, U_0^+ and U_0^- with their values a distance d from that point in the +z direction, U^+ and U^- (Fig. 2). For a given medium, the relationships among these quantities are

$$\begin{bmatrix} U_0^+ \\ U_0^- \end{bmatrix} = L \begin{bmatrix} U^+ \\ U^- \end{bmatrix}$$

where the amplitude transfer matrix is

$$L = \begin{bmatrix} \exp(-i\delta) & 0 \\ 0 & \exp(i\delta) \end{bmatrix}. \tag{17}$$

The quantity δ depends on the optical index n and the incident angle of the beam on the first surface of the stack (Appendix B).

Note that the quantities **n**, α, A, U, U^+, U^-, S, t, r, ξ, L, and δ all contain phase information and are, consequently, complex numbers.

3.1.5 The Transmittance and Reflectance of a Beam Incident on Thin Films Deposited on a Substrate in the Case of Phase Coherency Within the Film Layers

A stack configuration often encountered experimentally is that of a series of uniform films deposited on one or both sides of a substrate (Fig. 3). Using the transfer matrices in Eqs. (15) and (17), a researcher can calculate the transmitted and reflected amplitudes of the electromagnetic fields of a beam incident on the stack, if the film thicknesses and the complex indices of each film and those of the incident and exit media are known. From these amplitudes, one is able to find the absolute transmittance and reflectance of the beam for either mode and for an unpolarized beam (Appendix B).

We distinguish two cases of reflectance and transmittance depending on whether or not interference effects occur in the substrate.

3.2 OPTICAL MODEL IN THE CASE OF PHASE INCOHERENCY THROUGHOUT THE STACK

The transfer matrices applicable to a beam traversing a stack in which there is no interference relate beam intensities at various places in the stack and contain no complex numbers. We must, however, continue to distinguish between the modes of the incident beam as in Sections 3.1.1 and 3.1.2 above (Appendix C).

3.2.1 Phase Incoherent Transfer Matrix at an Interface of Two Media

Suppose I_j^+ represents the beam intensity in the jth medium going in the +z direction at the interface of the jth and mth media, and I_j^- is the beam intensity in the -z direction. If I_{0m}^+ and I_{0m}^- are the corresponding intensities of the beam in the mth medium, the transfer matrix among these intensities is (Appendix C)

$$\begin{bmatrix} I_j^+ \\ I_j^- \end{bmatrix} = \Xi_{jm} \begin{bmatrix} I_{0m}^+ \\ I_{0m}^- \end{bmatrix},$$

where the intensity transfer matrix Ξ_{jm} is

$$\Xi_{jm} = \frac{1}{T_{jm}} \begin{bmatrix} 1 & -R_{mj} \\ R_{jm} & (T_{jm}T_{mj} - R_{jm}R_{mj}) \end{bmatrix}. \tag{18}$$

The transmittance (T_{jm}) and reflectance (R_{jm}) coefficients come from the Fresnel amplitude coefficients (Eq. (16)),

$$T_{jm} = t_{jm}{}^{*}t_{jm}\left[\mathrm{Re}\left(\xi_m^{-1}\right)/\mathrm{Re}\left(\xi_j^{-1}\right)\right] \tag{19}$$

where Re indicates the real part of a complex number and

$$R_{jm} = r_{jm}{}^{*}r_{jm}.$$

3.2.2 Phase Incoherent Transfer Matrix Through a Uniform Medium

The phase incoherent transfer matrix ζ between the intensities, I_0^+ and I_0^- at the entrance surface of a uniform layer and the corresponding intensities, I^+ and I^-, at the layer's exit surface is (Appendix C)

$$\begin{bmatrix} I_0^+ \\ I_0^- \end{bmatrix} = \zeta \begin{bmatrix} I^+ \\ I^- \end{bmatrix},$$

and

$$\zeta = \begin{bmatrix} \exp\left(2\mathrm{Im}\left[\delta\right]\right) & 0 \\ 0 & \exp\left(-2\mathrm{Im}\left[\delta\right]\right) \end{bmatrix}. \tag{20}$$

Im refers to the imaginary part of a complex number.

3.2.3 The Transmittance and Reflectance of a Beam Incident on Thin Films Deposited on a Substrate in the Case of Phase Incoherency Throughout

The transmittance T and reflectance R of a beam incident upon a layered system of films on a substrate come directly from the intensity transfer matrices Ξ_{jm} and ζ in the case there is interference in any film or the substrate (Appendix C). As in the phase coherent case, the transmittance and reflectance of waves in the TE mode differ from those in the TM mode.

3.3 COMPUTER PROGRAM STACK

The model of the transmittance T and reflectance R of a light beam incident on a stack of uniform, homogeneous, layered materials consisting of films on either, or both, sides of a substrate is used in the computer program STACK to compute T and R. To use STACK, one needs the incident beam angle and the indices and the thicknesses of each film of the layered system and the substrate.

STACK users can select one of three coherence cases:

1. Interference occurs in all films and the substrate.

2. Interference occurs in all films but not in the substrate.

3. No interference takes place in any film or the substrate.

STACK is written in the Interactive Data Language (IDL) and is a replacement for program CALCRT (AEDC Technical Memorandum Report of May 1986), which calculates T and R for a beam incident on a single film on a substrate (See Appendix D). The model of a single film on a substrate is also used in AEDC program TRNLIN (Ref. 7) which finds the optical indices of a film from normal transmittance measurements of an incident beam. To date no AEDC programs exist which compute, from transmittance measurements, the optical indices for a film which is stacked with other films on a substrate.

4.0 EXAMPLES OF ANALYSES OF OPTICAL DATA OF MIXTURES

For the past several years, AEDC researchers have measured the infrared optical constants of many materials condensed on cryogenically cooled substrates. Some of the data are for the pure form of materials at different temperatures (and densities), and some are measurements of the optical properties of mixtures of these pure materials (Refs. 2-5, 8, and 9). We have used these data to illustrate the Lorentz-Lorenz transformation of the optical constants of a single material and some analysis methods for the optical properties of mixtures of materials.

4.1 LORENTZ-LORENZ TRANSFORMATIONS OF n OF A GIVEN MATERIAL AT DIFFERENT DENSITIES

The Lorentz-Lorenz constant of Eq. (5) allows researchers to compute the optical constants of a pure material at one density from their values at another density. We applied the Lorentz-Lorenz transformation to the optical constants measured at AEDC for three pure materials (CO_2, H_2O, and NH_3) which had formed cryofilms on a germanium (Ge) substrate at two temperatures, 20K and 80K. Consequently, we could calculate the optical constants of each material at 80K from their values at 20K and check the calculated values against the measured 80K values. We, of course, could go the other way and compute 20K values of the indices from the measured 80K values and compare with those actually observed at 20K.

4.1.1 The Lorentz-Lorenz Transformation

The transformation of the complex optical index **n** of a material with a (mass) density r to the optical index **n′** that the material has when its density is r′ comes from the fact that the Lorentz-Lorenz constant (Eq. (5)) must not change when the primed quantities replace the unprimed ones. We assume that the local field parameter b does not differ with density. Equating the primed and unprimed Lorentz-Lorenz constants, one can find **n'** from

$$n'^2 = \frac{\mathbf{n}^2\left(1 + b\frac{\rho'}{\rho}\right) + b\left(1 - \frac{\rho'}{\rho}\right)}{\mathbf{n}^2\ 1 - \frac{\rho'}{\rho} + b + \frac{\rho'}{\rho}}. \tag{21}$$

The computer program LLTRNSFM, written in IDL, uses Eq. (21) to compute the n and k spectra of a material at a given density from the measured n and k spectra at a different density.

4.1.2 Lorentz-Lorenz Transformations of the Optical Constants of CO_2 Films

Researchers at AEDC have observed the infrared n and k spectra of CO_2, H_2O, and NH_3 films formed on a Ge substrate at 20K and also at 80K. They used program TRNLIN to find least-squares values of the optical constants from normal transmittance measurements and then converted the least-squares k spectrum to an n spectrum via the subtractive Kramers-Kronig transformation in program SKKK2N,

$$\mathrm{n}(\nu) = \mathrm{n}(\nu_m) + \left(\frac{2}{\Pi}\right)\mathrm{P}\int_0^\infty \left[\frac{\nu'\mathrm{k}(\nu') - \nu\mathrm{k}(\nu)}{\nu'^2 - \nu^2} - \frac{\nu'\mathrm{k}(\nu') - \nu_m\mathrm{k}(\nu_m)}{\nu'^2 - \nu_m^2}\right] d\nu'. \tag{22}$$

ν_m is a reference wave number, and P denotes the Cauchy principal integral value.

4.1.2.1 Transformation of n of CO_2 from 20K to 80K

The authors transformed the 20K Kramers-Kronig n values of CO_2 and its least-squares k values to those n and k spectra that the Lorentz-Lorenz transformation predicts at 80K. The density of the CO_2 films was 1080 kg/m^3 at 20K and 1670 kg/m^3 at 80K (Table 1).

The transformed (Lorentz-Lorenz) n spectrum (for b = 2) near the strong $^{12}CO_2$ at 2350 cm^{-1} appears in Fig. 4 along with the observed (Kramers-Kronig) values of n observed at 80K; the analogous transformed and observed (least-squares) k spectra are in Fig. 5. Away from strong absorption bands, the transformed and observed n values are in good agreement. However, the

peak value of k (Lorentz) is shifted downward in wave number from the measured k peak, and the extrema of n (Lorentz) are displaced to lower wave numbers from those observed for n at 80K. In addition, the peak of the Lorentz-Lorenz value of k is greater than its measured value, and the deviations in the Lorentz-Lorenz n spectrum are more than the deviations observed for n at 80K.

To check the effect of measurement errors in the density values of the CO_2 films, we recalculated the Lorentz-Lorenz spectra with new density values and noted that as the ratio of the densities, ρ (80K)/ ρ (20K), decreases towards unity, the spectral shifts lessened but the agreement between the n spectra away from the strong band worsened. We conclude from this, and other examples, that the better the n values (away from strong absorptions) agree, the more confidence we have that the density values are correct.

We also experimented with the value of the local field parameter b and found, to our surprise, that if just the value of b is changed from 2 to 10^{20} (essentially infinity), the n and k spectra resulting from the transformation agree surprisingly well with the corresponding observed spectra (Figs. 6 and 7). This means, by Eq. (2), that parameter a in Eq. (3) is zero in this example. Thus, in contrast to the normal assumption for non-polar lih dielectrics (where $a = 3/\varepsilon_0$ and $b = 2$), the present result indicates that the (average) contribution of the polarization vector $\vec{P}$ to the local electric field $\vec{E}_{loc}$ within the dielectric is negligible for CO_2 films.

4.1.2.2 Transformation of n of CO_2 from 80K to 20K

The n and k spectra that come from a Lorentz-Lorenz transformation of 80K n and k data to their values at 20K are pictured in Figs. 8 and 9. In contrast to the 20K to 80K transformation, the Lorentz-Lorenz spectra have shifts upward in wave number, and the peak values of k and n are smaller than those experimentally observed. As in the 20K to 80K transformation, the spectral shifts decrease as the ratio of the densities decreases toward one, but the n values away from the strong absorption band diverge. Again, when the value of b is 10^{20}, the corresponding transformed and observed spectra become more alike (Figs. 10 and 11).

4.1.3 Lorentz-Lorenz Transformations of the Optical Constants of H_2O Films

We applied the above analysis techniques for CO_2 to 20K and 80K n and k spectra of H_2O films. The density of 20K film (670 kg/m^3) is again greater than the 80K film density (920 kg/m^3) (Table 1).

4.1.3.1 Transformation of n of H_2O from 20K to 80K

The Lorentz-Lorenz transformed n and k spectra (from 20K to 80K) are compared to the corresponding observed values in Figs. 12 and 13. Though the two k spectra are close in the strong absorption band centered near 3300 cm^{-1}, they differ greatly in the 1200 to 2800 cm^{-1} and 750 cm^{-1} regions, and the transformed n spectrum is everywhere greater than the observed one. By adjusting the values of either the densities or of the parameter b, one can get closer agreement in certain regions of the spectra but at the expense of worse agreement in other regions. The cause for this may be that the physical structure of the H_2O films is different at the two temperatures much like the case of NH_3 films. (See Section 4.1.4 below.) It is also possible that the analysis methods need revision or the original measurement and data reduction procedures are in error.

4.1.3.2 Transformation of n of H_2O from 80K to 20K

Figures 14 and 15 compare the transformed n and k spectra to the observed ones when going from 80K to 20K. Again, the agreement between the k spectra is best near 3300 cm^{-1}, but poor elsewhere, and the n spectra are not close anywhere. No value of the parameter b allows better agreement everywhere in the spectra; the same is true for the densities.

4.1.4 Lorentz-Lorenz Transformations of the Optical Constants of NH_3 Films

The Lorentz-Lorenz n and k spectra and the corresponding observed spectra for NH_3 films are in Figs. 16 and 17 for the 20K to 80K transformation and in Figs. 18 and 19 for the 80K to 20K transformation. The film density at 20K (670 kg/m^3) is, as for the two film materials above, less than that at 80K (920 kg/m^3).

Because the absorption bands measured for the 80K films are much stronger and sharper than those measured at 20K, the transformed k spectra bear little resemblance to the observed k spectra. However, except near the bands at 1100 cm^{-1} and 3350 cm^{-1}, the n spectra agree well. Varying b or the density values does not change the computed k spectra enough to mimic the observed k spectra.

The major reason for this nonagreement between the 20K and 80K NH_3 spectra is that the structure of the 80K film was crystalline while that of the 20K film was amorphous or metastable (Ref. 10). This accounts for the stronger and narrower features in the experimental 80K spectra compared to those in the 20K spectra; the Lorentz-Lorenz transformation does not change significantly the sharpness of the peaks.

4.1.5 Discussion of Lorentz-Lorenz Transformation Results

The results of the Lorentz-Lorenz transformation for CO_2 films show that this analysis method may yield n and k spectra similar to those actually measured at a different density provided the film material is predominantly made of molecules which do not form hydrogen bonds, and the proper value of the local field parameter b is used. For films composed of hydrogen-bonding molecules like H_2O and NH_3, the physics is more complicated than the simple changes of the optical constants that density differences alone can create. To create an adequate model, one probably must look in (quantum mechanical) detail at the microstructure of films of hydrogen-bonding molecules and the changes that occur because of different condensation temperatures, molecular migration rates, annealing effects, and so forth.

4.2 LORENTZ-LORENZ ANALYSIS METHODS OF THE OPTICAL PROPERTIES OF MIXTURES OF MATERIALS

One of the goals of the AEDC research program on contaminants of spacecraft is to predict the optical properties of a film composed of a mixture of materials from the known optical indices of each component material. In this section, we calculate optical constants of several cryogenic films which are mixtures of some simple molecules, with the help of the Lorentz-Lorenz result of Eqs. (8) and (9), and compare these indices with the n and k spectra measured for the mixture.

We also compared the computed transmittance spectra of selected films of mixtures with their computed transmittance spectra calculated with measured optical constants of the mixture and some spectra computed as if the components of the mixture formed separate layers within the larger film. To compute the last spectra, we must decide what thickness value each layer might have and in what order are the layers of the film, none of which comes from experimental data. We make the assumption that each density, ρ_i that component i has in its layer of the film is related to its density ρ_{pi} in its pure state by the same factor as any other component; that is, $\rho_i = \beta\rho_{pi}$, where β is constant for all components i. When we combine this assumption with the fact that the sum of the thickness values, d_i, of each layer must be the (measured) value of the total film thickness d, we have

$$d_i/d = (M_i/M)\,(\rho/(\beta\rho_{pi}))\,,$$

where

$$\beta = (S\,(M_i/M)\,(\rho/\rho_{pi}))\,. \tag{23}$$

Here, M_i/M is the mass ratio of the ith component and ρ is average density, respectively, of the film. (If the mole fractions, N_i/N, are known instead of mass ratios, we can use the conversion,

$M_i/M = (N_i/N)(m_i/m)$, where m_i/m is the molecular mass ratio of the ith component to the average molecular mass of the components.)

We also assumed that the film component whose pure state equilibrium vapor pressure was the lowest, at a given substrate temperature, would form the first layer on the substrate; the component with the next lowest vapor pressure would form the next layer on top of the first layer; and so forth. Thus, by the above criterion, for a $N_2/H_2O/CO_2/CO$ film structured in layers, the order of the layers (starting with the side on which the beam is incident) is CO, N_2, CO_2, and H_2O.

4.2.1 Optical Properties of 20K 50-Percent CO_2/50-Percent CO Films

Several years ago, researchers at AEDC measured the optical properties of films made of small molecules condensed onto a Ge substrate at 20K or 80K (Ref. 5). We used these data in program NMIX to compute the optical constants of 20K films composed of 50-percent (mole fraction) CO_2 molecules and 50-percent CO molecules and to compare to the measured n and k spectra; all b values were set to 2. The measured and computed n and k spectra appear, respectively, in Figs. 20 and 21. Except near the large CO_2 absorption band at 2350 cm^{-1}, the calculated and measured n spectra are close, though usually the calculated n values are greater than the corresponding measured values. Both the n and k spectra are shifted slightly from one another near 2350 cm^{-1}.

The measured k spectrum is smaller than the corresponding calculated one at the large CO_2 band but greater at the 2150 cm^{-1} CO band. This may mean that the concentration of CO_2 molecules is less than 50 percent. (However, when the mole fraction of CO_2 is set to 40 percent, so that the new calculated k spectrum nearly matches the measured spectrum near the CO_2 band, at the CO band near 2150 cm^{-1} the measured k values are still much greater than the calculated ones.) Likewise, making small changes in the values of b improves the agreement of the calculated n and k spectra with the measured spectra, but, in contrast to the case of pure CO_2 films discussed above, when b is set to 10^{20}, the calculated spectra are highly distorted from the measured ones.

Figure 22 is a plot of three computed normal transmittance infrared spectra for a 13.16-μm CO_2/CO on a 20K Ge substrate. The spectrum labeled "T (obs)" is calculated from the measured optical constants of the mixture (Ref. 5); "T (mix)" is computed from the calculated optical constants (from program NMIX) of the mixture; and "T (layers)" is a STACK calculation of the transmittance as if a uniform 6.08-μm CO layer were next to a 7.08-μm layer of CO_2 which is on the substrate. T (mix) and T (layers) are nearly identical, which may seem surprising because in the latter case, there are actually two films stacked on the substrate, and multiple reflections can occur at their mutual interface. Nevertheless, the interference fringes of these two spectra mimic one another. This is probably because the refractive indices of each of the layers are close to each other in value and that of Ge is several times greater. The period of the T (obs) spectrum is notice-

ably greater than those of T (mix) and T (layers) and indicates the refractive index of the observed film is less than that calculated in NMIX. These spectra are very similar to the measured spectrum found in Fig. 11 of Ref. 5.

4.2.2 Optical Properties of 20K 64-Percent N_2/23-Percent CO/13-Percent CO_2 Films

When N_2, which has no near infrared absorption bands, is added to the mixture of CO and CO_2, the expected n, k, and T spectra are similar to those of the CO_2/CO films. Indeed this is the case, as Figs. 23, 24, and 25 show for n, k, and T, respectively.

Away from the CO_2 band at 2350 cm^{-1}, the calculated n values roughly agree with the measured values, though they are greater over most of the spectrum. The extrema of the measured n spectrum are much more pronounced near the CO_2 band and are shifted from the calculated values as well. The measured k spectrum has peak values greater than the calculated ones at the 2150 cm^{-1} CO band and at 2350 cm^{-1}. The differences in the calculated n and k spectra from the measured spectra indicate that the concentrations of both CO and CO_2 molecules may have been higher than 23 percent and 13 percent, respectively. (The mole fractions were found from chemical analysis of the gaseous mixture used to make the film deposit. The actual composition of the film on the substrate cannot be measured directly.)

In Fig. 25, the T (layers) spectrum is calculated in STACK as if the 6.602-μm film had a uniform CO layer 1.521 μm thick at its outer surface (closest to the source of the infrared beam), a 1.001-μm layer of CO_2 next to the substrate, and a 4.080-μm N_2 layer sandwiched between them. Again, it is noteworthy that though interference effects can occur within each layer, the interference fringe pattern has a structure and a period that is very much like the one in the T (obs) spectrum in which the observed film optical constants were used and the deposit was treated as a single film. The single film calculation using the optical constants from NMIX produced a spectrum "T (mix)" which has a fringe period less than those of the other two. This indicates the values of n from NMIX are greater than the observed values and may be the result of possible errors in the concentration values of the components mentioned above. The measured T spectrum of the film (Fig. 13 of Ref. 5) has features that are most like those of T (obs).

4.2.3 Optical Properties of 20K 50.3-Percent N_2/22.5-Percent H_2O/17.2-Percent CO_2/10.0-Percent CO Films

Our last example of a 20K film is a mixture of the components of the last film material, N_2, CO_2, and CO, with H_2O molecules that can form hydrogen bonds with other molecules. (This mixture is named "Simulated Plume Mixture 1" in Ref. 5.) The n, k, and T spectra of these films appear, respectively, in Figs. 26, 27, and 28.

In most spectral regions away from the CO_2 band at 2350 cm^{-1}, the calculated n and measured n spectra are in good agreement. Near 2350 cm^{-1}, the peaks of the calculated k spectrum are much less than those measured, and the calculated peak is shifted upwards in wave number from 2346 to 2360 cm^{-1}. However, the calculated peak k values at the water band near 3300 cm^{-1} are much greater than the measured peaks. There are at least two causes for these discrepancies between spectra. First, the concentration values of the absorbing molecules may be in error. (It appears that the concentration of CO_2 may be higher than 17.2 percent, and that of H_2O may be lower than 22.5 percent.) Second, and probably more importantly, the degree of hydrogen bonding of the water molecules is highly dependent on its concentration (Ref. 5). As the concentration of H_2O molecules grows, the 3300 cm^{-1} O-H stretch band rapidly becomes more intense and wider in a nonlinear way. Evidently, for this film material the degree of hydrogen bonding is much less than that observed in pure H_2O films (Fig. 13).

The differences between the calculated and observed n and k spectra are evident in the calculated transmittance spectra of a 20K $N_2/H_2O/CO_2/CO$ film 6.72-μm thick that appear in Fig. 28. The spectrum calculated from observed film optical constants, T (obs), matches the measured spectrum very well (Fig. 21 of Ref. 5). That calculated from the optical constants computed in NMIX, T (mix), is similar to T (layers). (In the calculation of the T (layers) spectrum, the order of the layers is: CO (0.70 μm), N_2 (3.40 μm), CO_2 (1.40 μm), H_2O (1.21 μm), and Ge substrate.) The T (mix) and T (layers) spectra have stronger and broader H_2O bands than observed because their calculations are based on the optical constants of pure H_2O spectra where the degree of hydrogen bonding is at a maximum.

4.2.4 Optical Properties of 80K Films of a Mixture of Uralane® and RTV®-566

Our last example is a mixture of 47 percent (by weight) Uralane 5753-A/B (LV) urethane casting compound and 53 percent (by weight) RTV-566 silicon sealant ("Mixture 2" in Ref. 4). The measured and calculated n, k, and T spectra are in Figs. 29-31.

The calculated n spectrum is larger everywhere than the measured n spectrum; the calculated k spectrum is greater than measured k spectrum except at 3300 cm^{-1} where they are essentially identical. The T (obs)spectrum, computed from the observed optical constants, is in good agreement with the measured T spectrum, T (meas), though near 2000 cm^{-1} T (obs) is greater than T(meas). The T (mix) spectrum is less than the measured T spectrum, but they agree well at 3300 cm^{-1}. The agreement of the spectra can be improved by redoing the calculations with a slight change in the concentrations of the components. The T (layers) spectrum is for a uniform 0.894-μm layer of RTV-566 on a 0.692-μm layer that is next to the 80K Ge substrate. Of the three calculated spectra, it has the worse agreement with the measured T spectrum.

4.2.5 Discussion of the Lorentz-Lorenz Methods for Computing the Optical Properties of Mixtures

The Lorentz-Lorenz methods to predict the optical constants of a film composed of a mixture, whose optical constants in the pure state are known, can provide results which are accurate to within 10 percent, or so, away from strong absorption bands. One difficulty in getting more accurate predictions is the experimental error in the values of the concentrations of each film omponent. Other difficulties include the theoretical and experimental uncertainties of the effects of intermolecular attractions. All difficulties become more acute as the number of constituents in the mixture increases.

The problem of intermolecular attractions is compounded by the phenomenon of hydrogen bonding which affects many common molecules like H_2O and NH_3. Because spectral features change drastically as the degree of hydrogen bonding varies (Ref. 11), the optical constants of the pure state of hydrogen-bonding molecules do not have the spectral features needed for materials where the degree of hydrogen bonding is less. To predict the optical constants in these cases, one might use the optical constants measured for hydrogen-bonded molecules diluted in an inert matrix such as solid N_2 or Ar. For instance, a researcher might be able to use the optical constants of a film of the appropriate concentration of H_2O molecules in N_2 to predict more accurately the spectral features due to H_2O in the 20K $N_2/H_2O/CO_2/CO$ film (Figs. 26–28).

REFERENCES

1. Roux, J. A. and McCay, T. D., Eds. *Progress in Astronautics and Aeronautics, Spacecraft Contamination: Sources and Prevention.* American Institute of Aeronautics and Astronautics (AIAA), New York, 1984.

2. Wood, B. E., Bertrand, W. T., Bryson, R. J., Seiber, B. L., Falco, P. M., and Cull, R. A. "Surface Effects of Satellite Outgassing Products." AEDC-TR-87-8, September 1987. (Also *AIAA Journal of Thermophysics and Heat Transfer*, Vol. 2, No. 4, October 1988, pp. 289-295.)

3. Wood, B. E., Bertrand, W. T., Kiech, E. L., Holt, J. D., and Falco, P. M. "Surface Effects of Satellite Material Outgassing Products." AEDC-TR-89-2 (AD-B133593), June 1989.

4. Bertrand, W. T. and Wood, B. E. "Effects of Spacecraft Materials Outgassing Products on Cryogenic Surfaces." AEDC-TR-92-18 (AD-A262671), March 1993.

5. Palmer, K. F., Wood, B. E., and Roux, J. A "Infrared Optical Properties of Solid Mixtures of Molecular Species at 20°K." AEDC-TR-80-30 (AD-A094214), January 1981.

6. Potter, R. F. "Basic Parameters for Measuring Optical Properties." *Handbook of Optical Constants of Solids*, Palik, E. D., Ed. Academic Press, New York, 1985.

7. Pipes, J. G., Rous, J. A., Smith, A. M., and Scott, H. E. "Transmission of Infrared Materials and Condensed Gases at Cryogenic Temperatures." AEDC-TR-77-71 (AD-A044517), September 1977.

8. Roux, J. A., Wood, B. E., and Smith, A. M. "Infrared Optical Properties of Thin H_2O, NH_3, and CO_2 Cryofilms." AEDC-TR-79-57 (AD-A074913), September 1979.

9. Wood, B. E., and Roux, J. A. "Infrared Optical Properties of Thin CO, NO, CH_4, HCl, N_2O, O_2, N_2, and Ar Cryofilms." *Progress in Astronautics and Aeronautics, Spacecraft Contamination: Sources and Prevention*, Roux, J. A. and McCay, T. D., Eds. American Institute of Aeronautics and Astronautics (AIAA), New York, 1984.

10. Clapp, M. L. and Miller, R. E. "Shape Effects in the Infrared Spectrum of Ammonia Aerosols." *Icarus*, Volume 105, 1993, pp. 529–536

11. Palmer, K. F., Wood, B. E., and Roux, J. A. "Infrared Optical Properties of Solid Mixtures of Molecular Species at 20K." *Progress in Astronautics and Aeronautics, Spacecraft Contamination: Sources and Prevention*, Roux, J. A. and McCay, T. D., Eds. American Institute of Aeronautics and Astronautics (AIAA), New York, 1984

12. Guenther, G. D. *Modern Optics*. John Wiley & Sons, New York, 1990.

13. Born, M. and Wolf, E. *Principles of Optics*. Fifth Edition, Pergamom Press, Oxford, 1975.

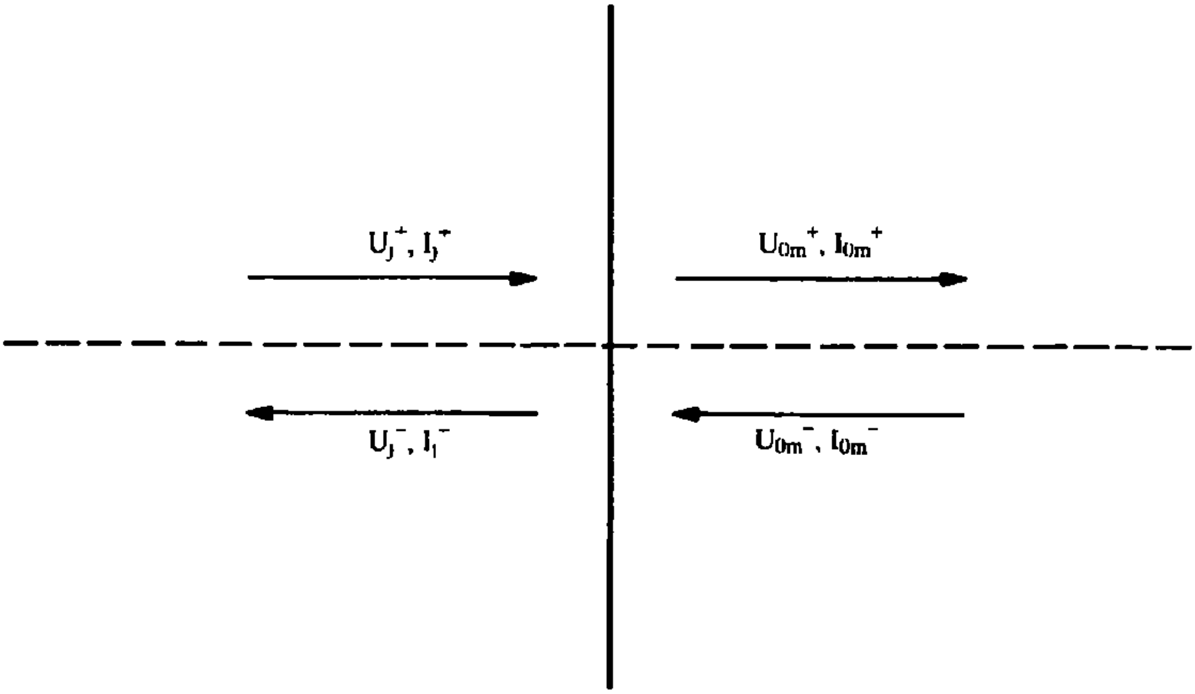

Figure 1. Amplitudes and intensities at an interface.

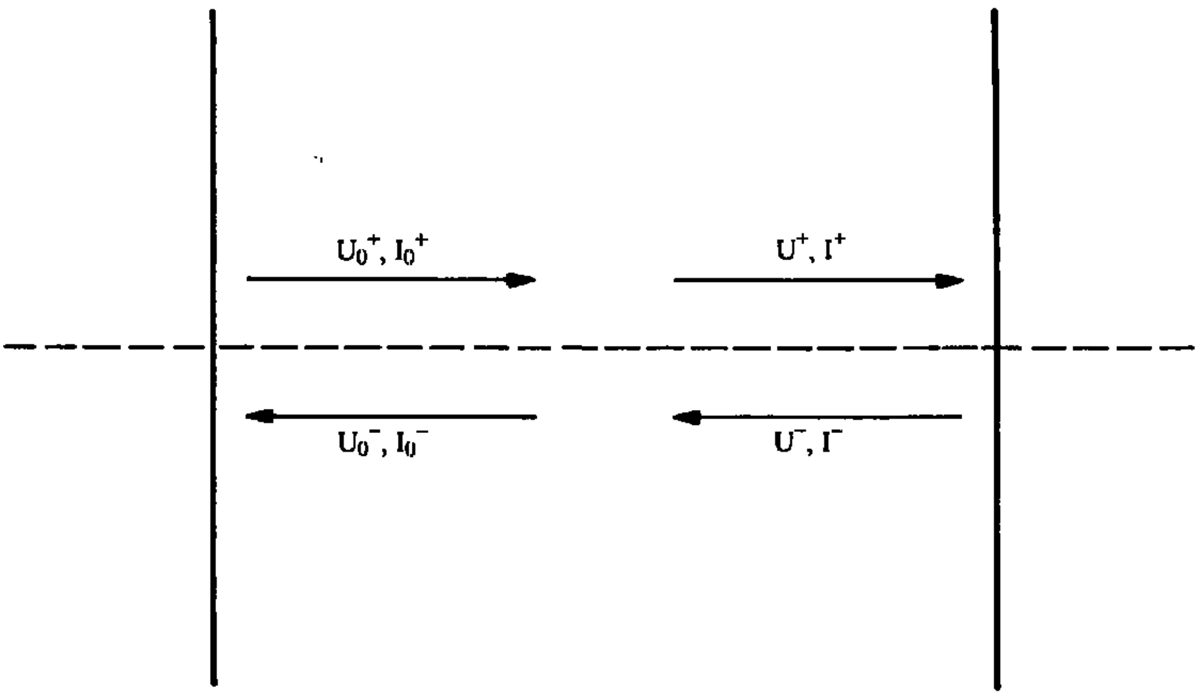

Figure 2. Amplitudes and intensities in a film medium.

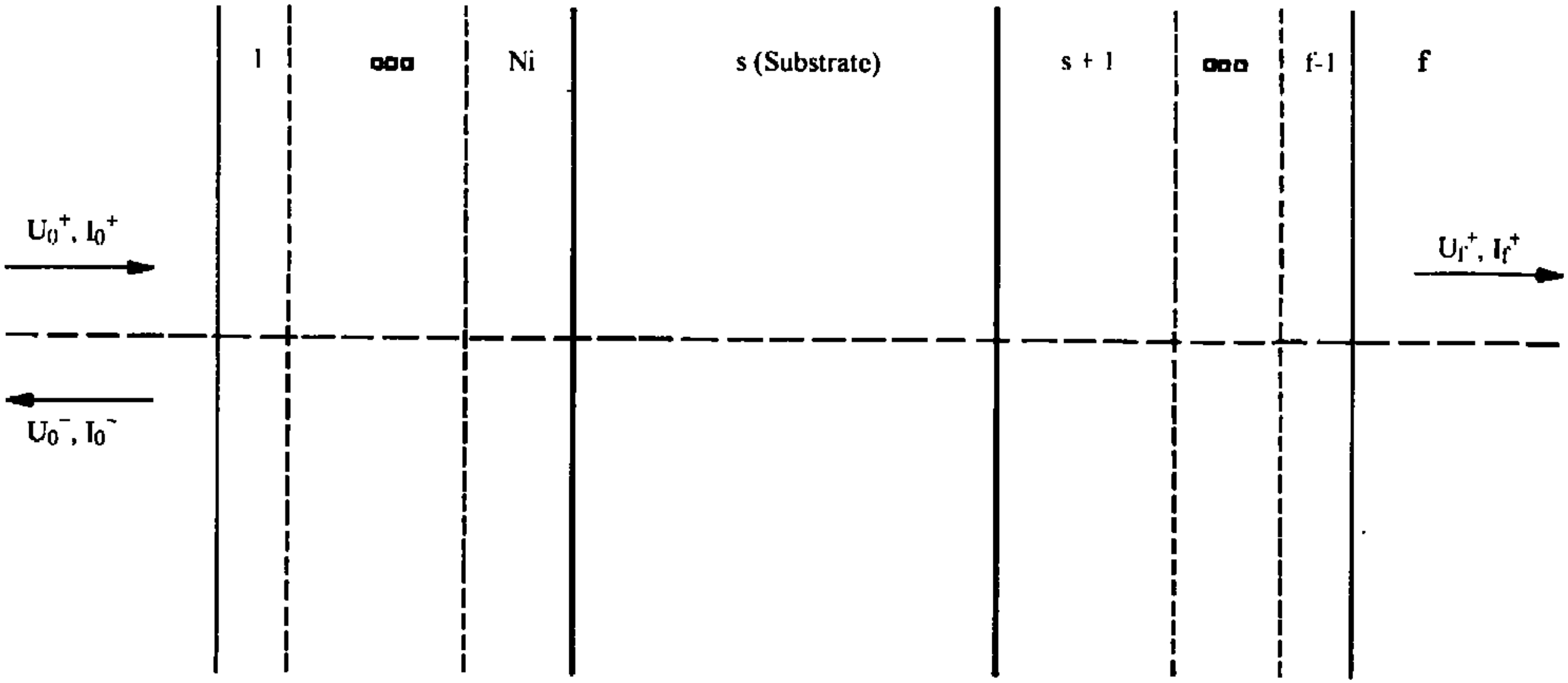

Figure 3. Stack of films on a substrate.

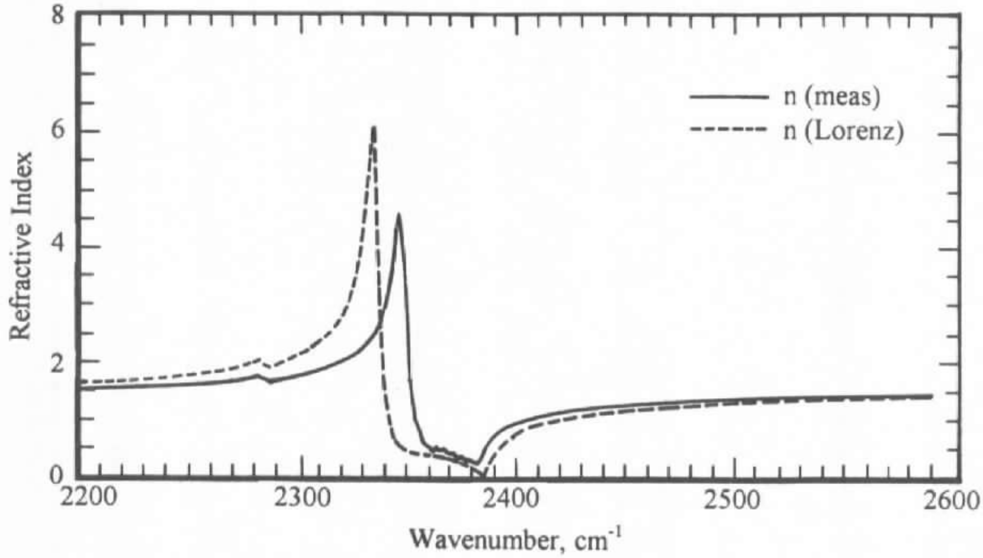

Figure 4. Lorentz-Lorenz transformation of n for CO_2 films (20K to 80K).

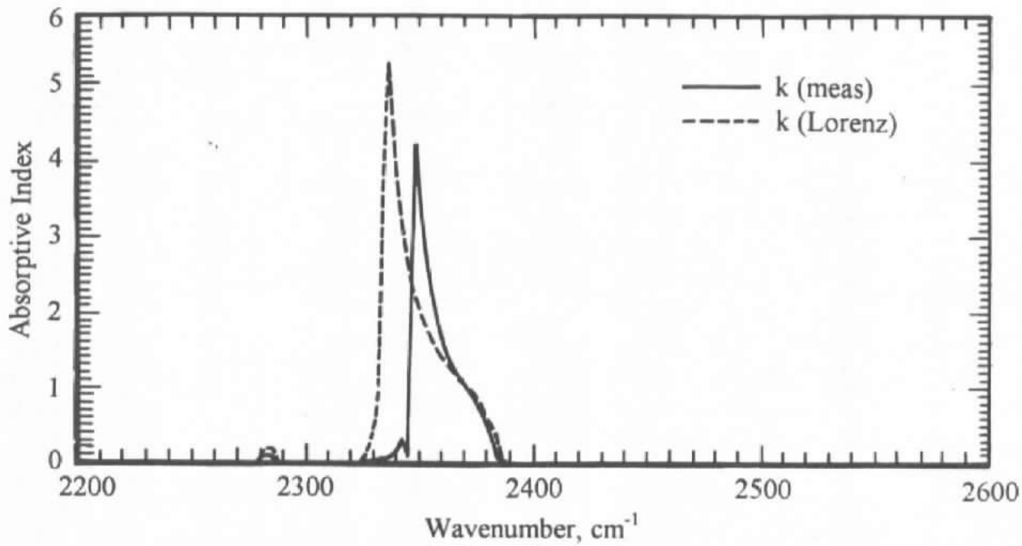

Figure 5. Lorentz-Lorenz transformation of k for CO_2 films (20K to 80K).

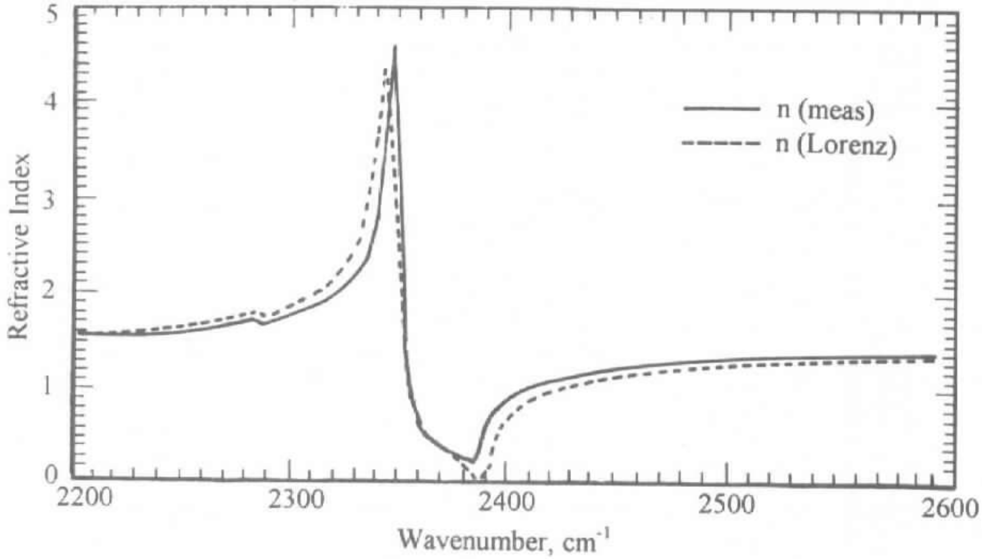

Figure 6. Lorentz-Lorenz transformation of n for CO_2 films (20K to 80K, b = 1.0E20).

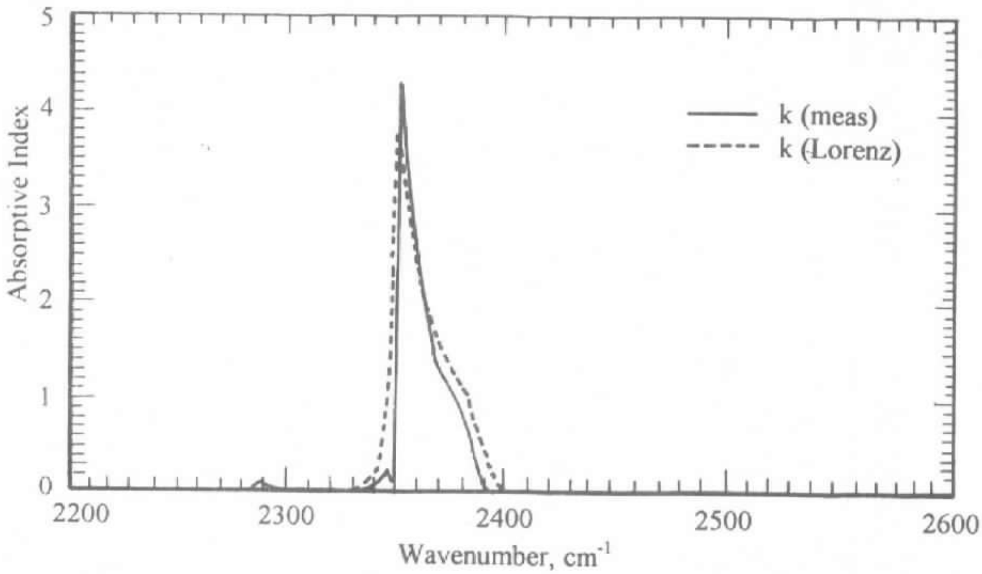

Figure 7. Lorentz-Lorenz transformation of k for CO_2 films (20K to 80K, b = 1.0E20).

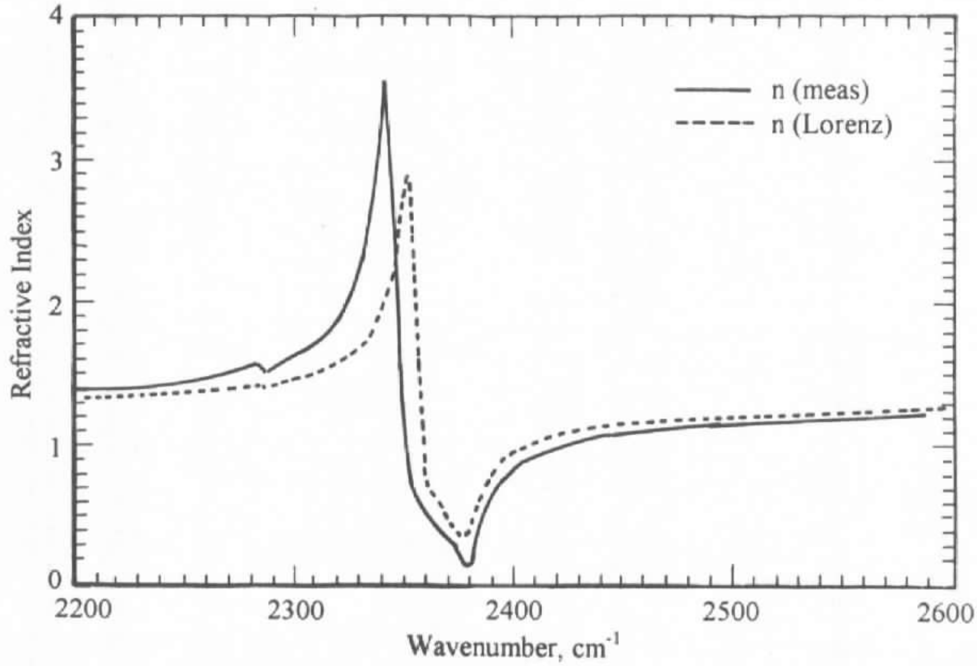

Figure 8. Lorentz-Lorenz transformation of n for CO_2 films (80K to 20K, b = 1.0E20).

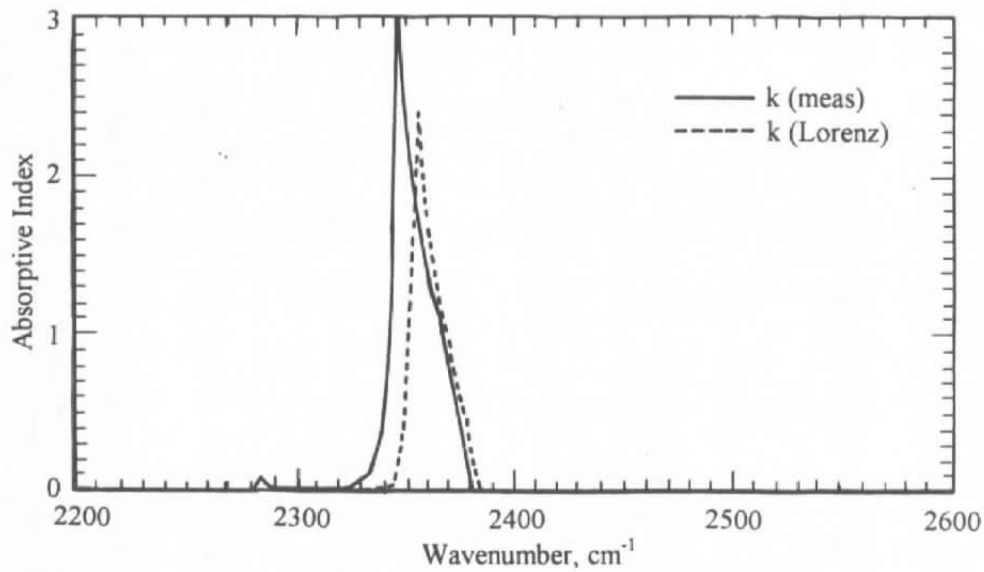

Figure 9. Lorentz-Lorenz transformation of k for CO_2 films (80K to 20K, b = 1.0E20).

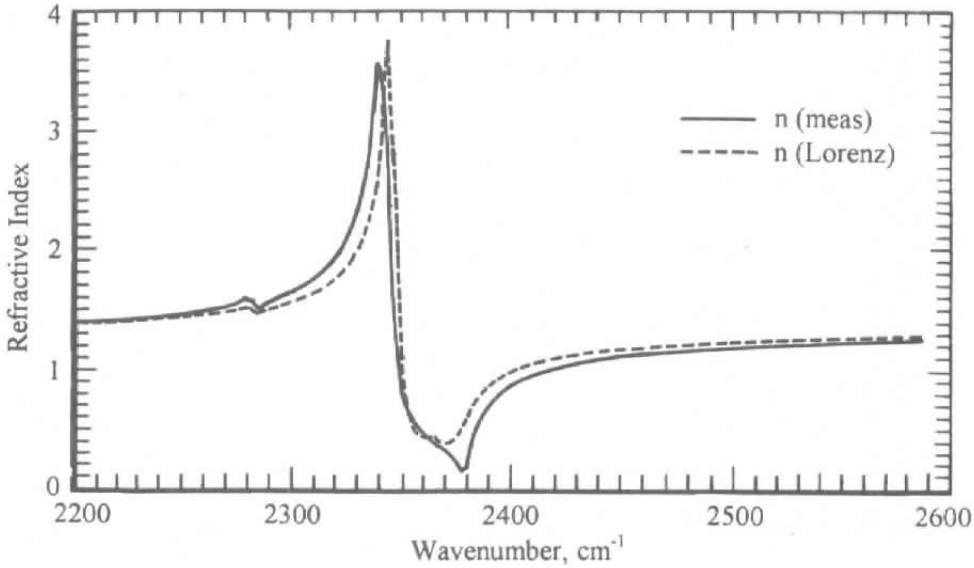

Figure 10. Lorentz-Lorenz transformation of n for CO_2 films (80K to 20K, b = 1.0E20).

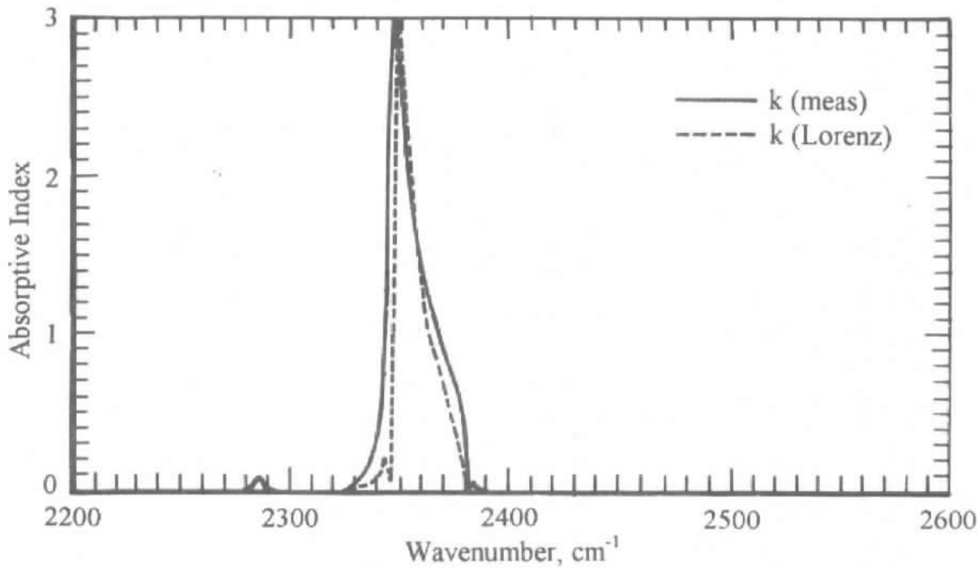

Figure 11. Lorentz-Lorenz transformation of k for CO_2 films (80K to 20K, b = 1.0E20).

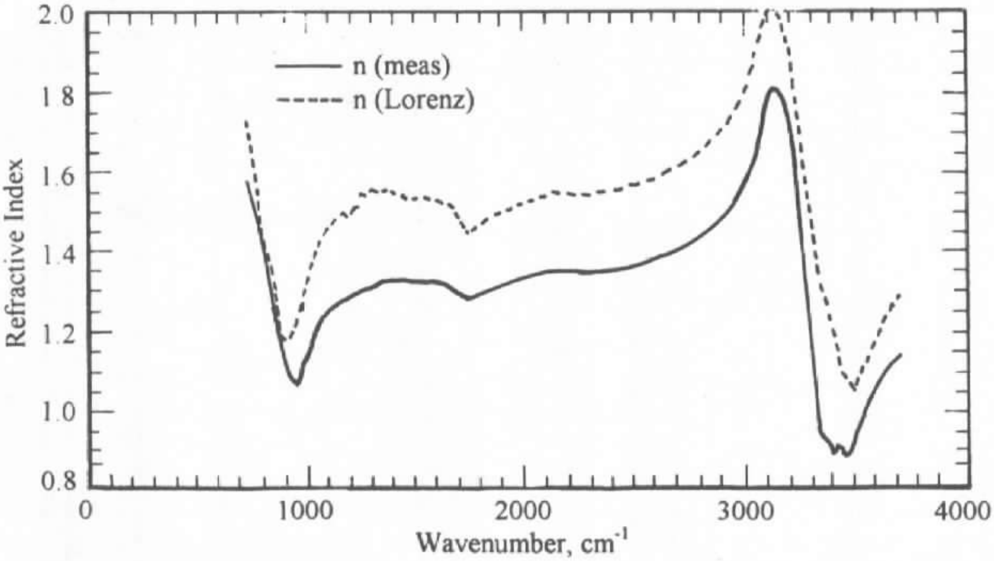

Figure 12. Lorentz-Lorenz transformation of n for H_2O films (20K to 80K).

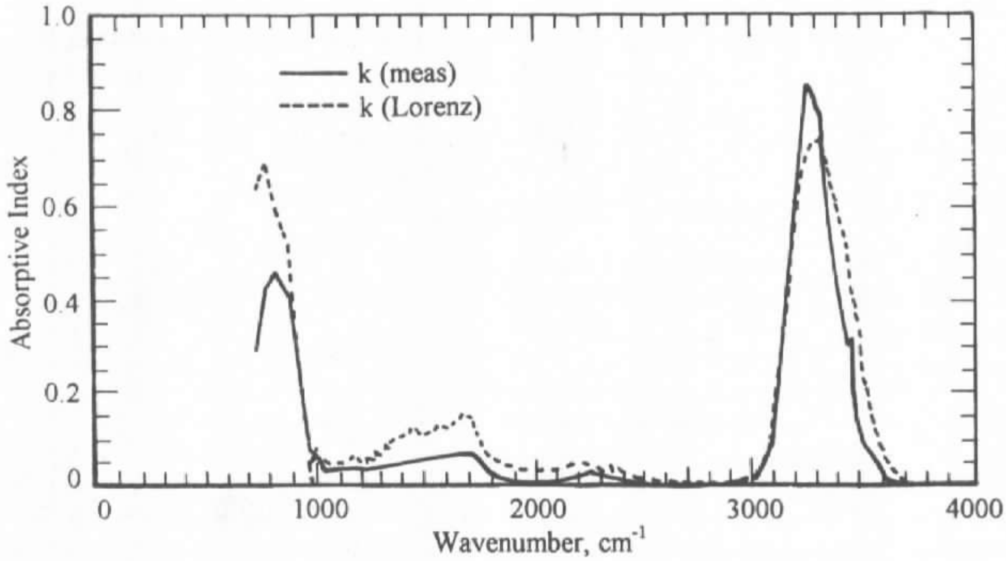

Figure 13. Lorentz-Lorenz transformation of k for H_2O films (20K to 80K).

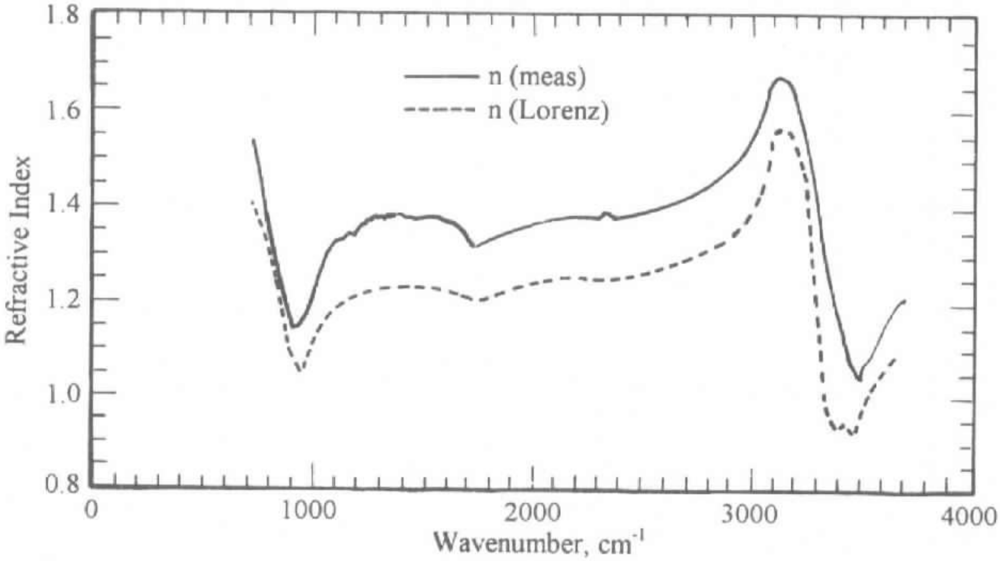

Figure 14. Lorentz-Lorenz transformation of n for H_2O films (80K to 20K).

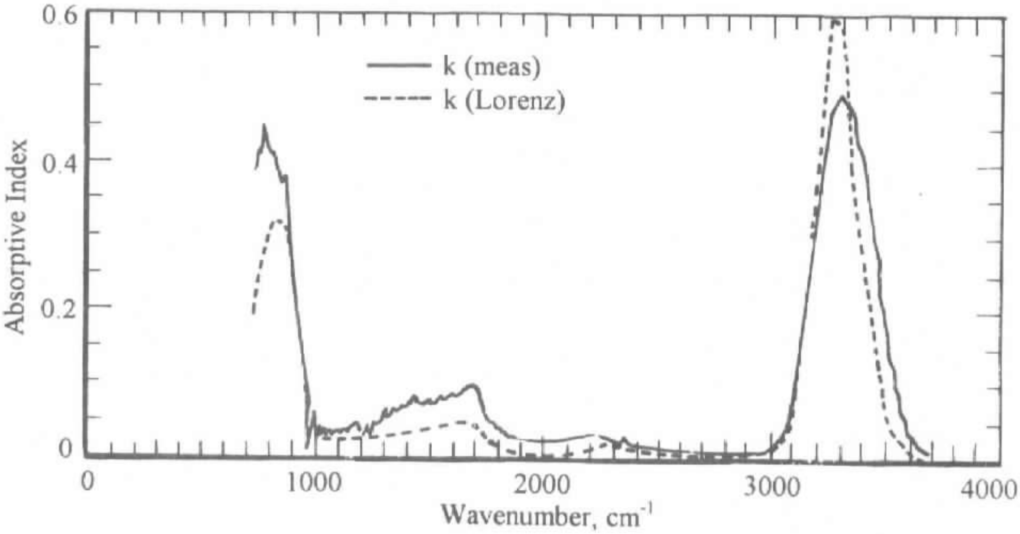

Figure 15. Lorentz-Lorenz transformation of k for H_2O films (80K to 20K).

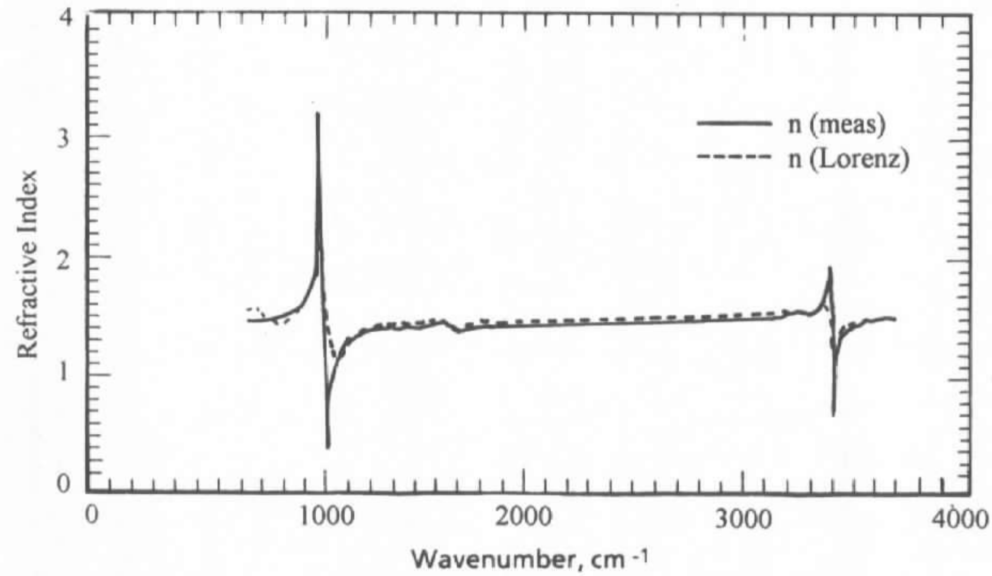

Figure 16. Comparison of n (meas) and n (Lorenz) of 80K NH_3 films (from 20K data).

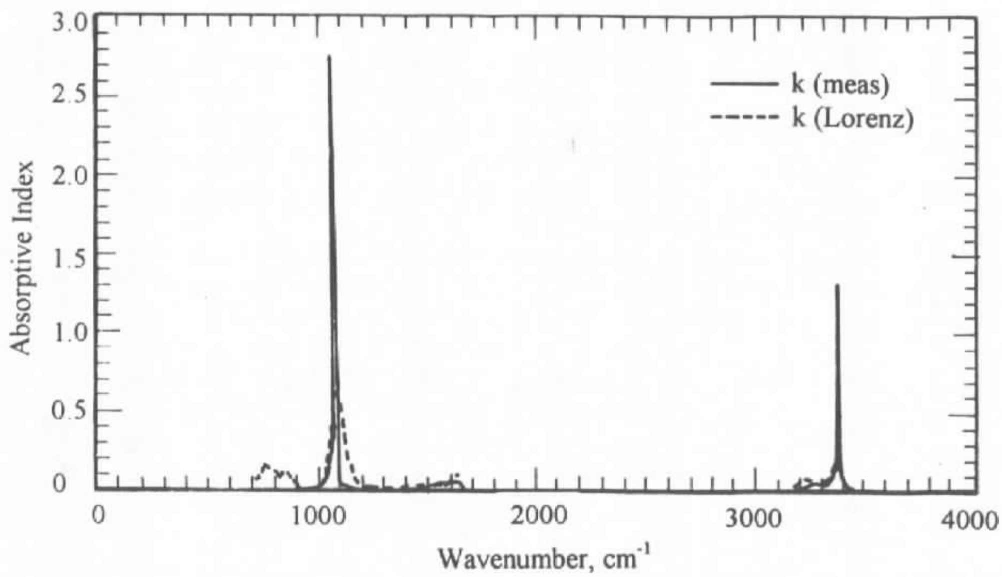

Figure 17. Comparison of k (meas) and k (Lorenz) of 80K NH_3 films (from 20K data).

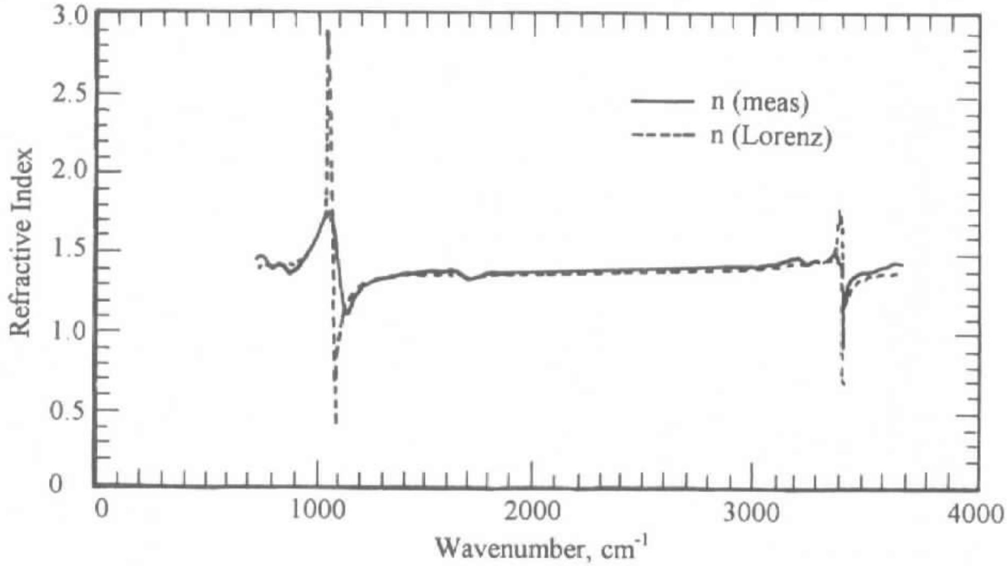

Figure 18. Comparison of n (meas) and n (Lorenz) of 20K NH_3 films (from 80K data).

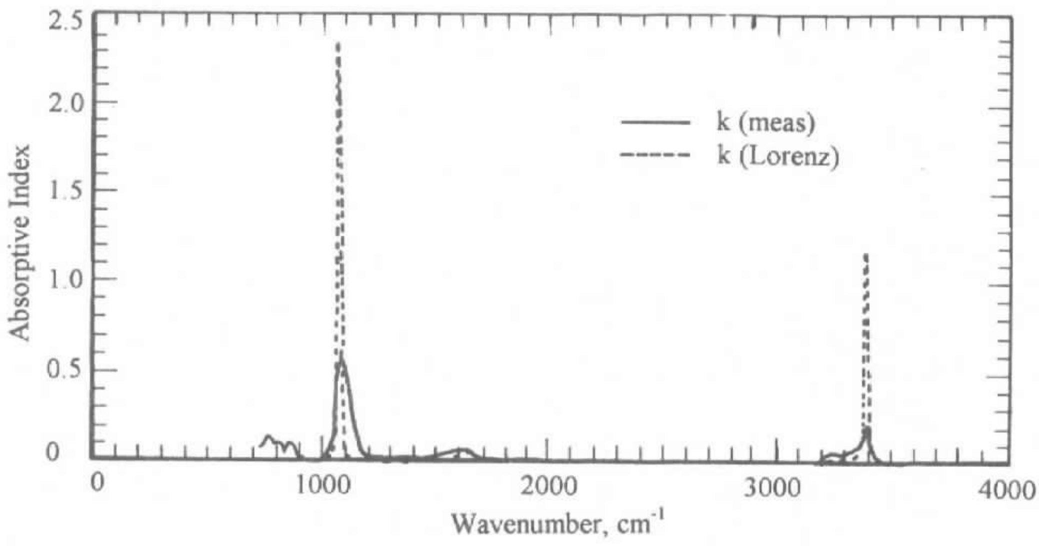

Figure 19. Comparison of k (meas) and k (Lorenz) of 20K NH_3 films (from 80K data).

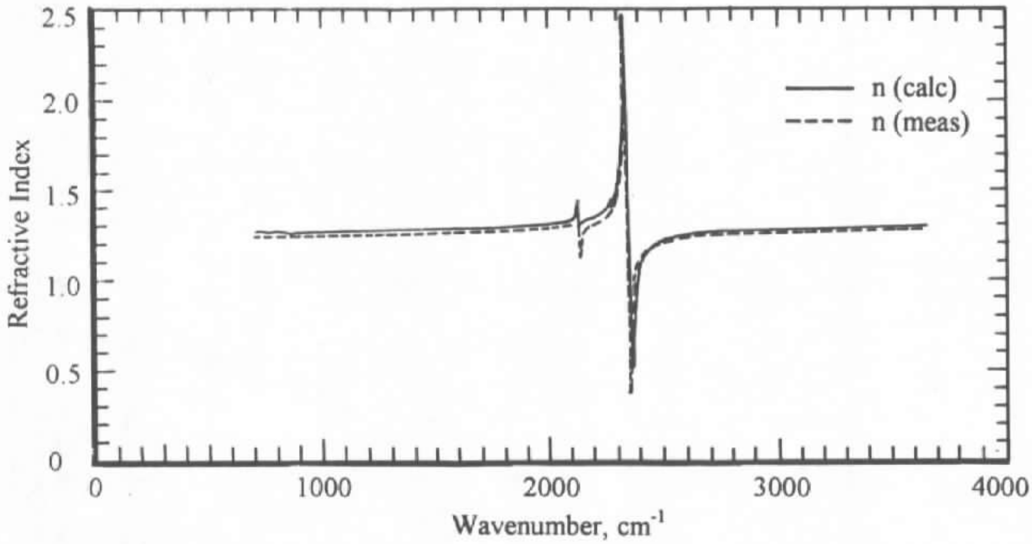

Figure 20. n (calc) and n (meas) of 20K CO_2/CO film.

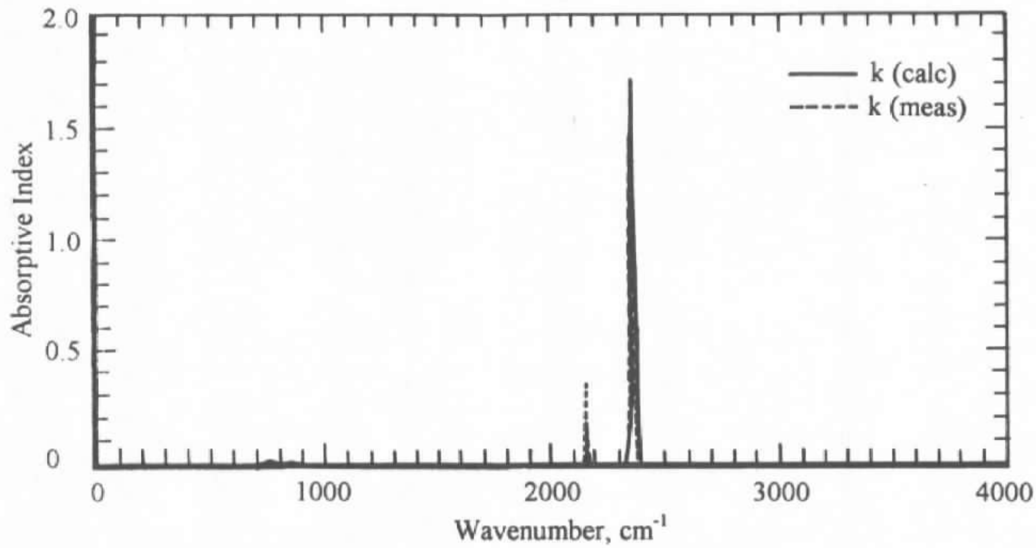

Figure 21. k (calc) and k (meas) of 20K CO_2/CO film.

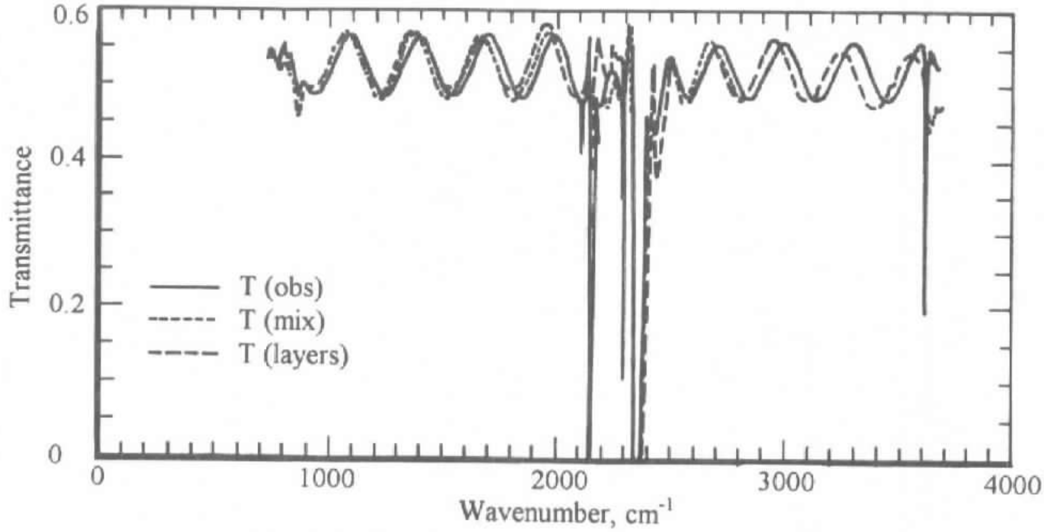

Figure 22. Calculated transmittance of 13.16-μm CO_2/CO film.

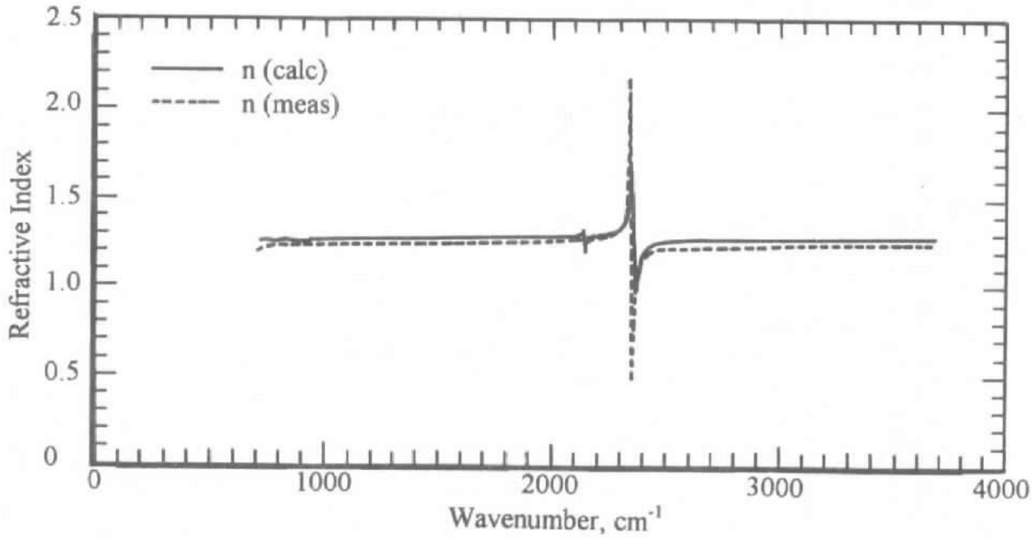

Figure 23. n (calc) and n (meas) of 20K N_2/CO/CO_2 film.

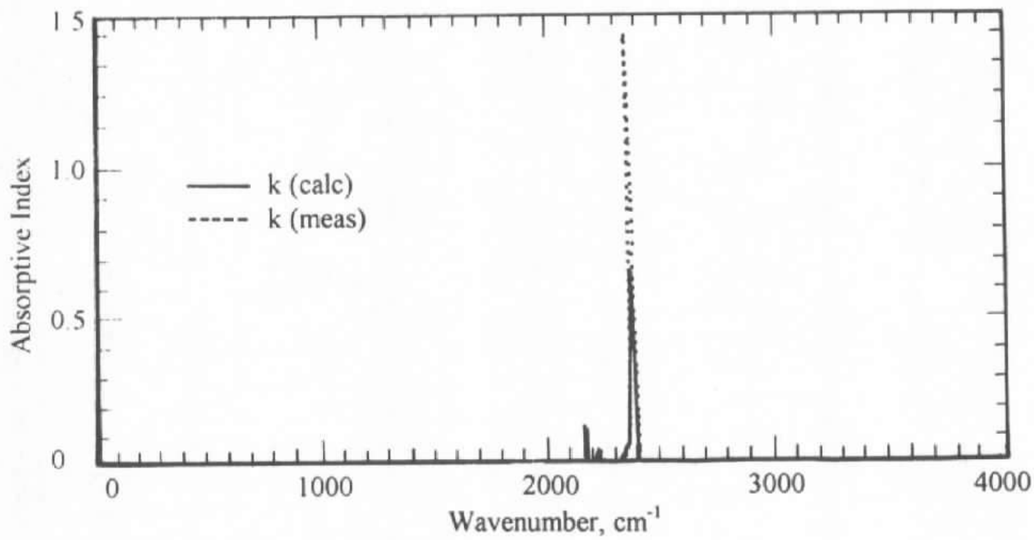

Figure 24. k (calc) and k (meas) of 20K $N_2/CO/CO_2$ film.

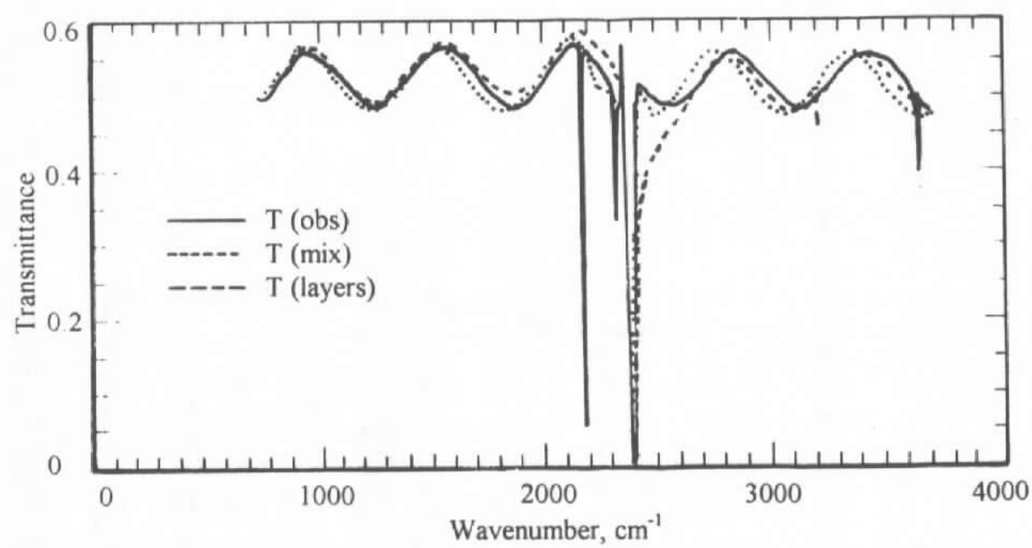

Figure 25. Calculated transmittance of 6.602-μm $N_2/CO/CO_2$ film.

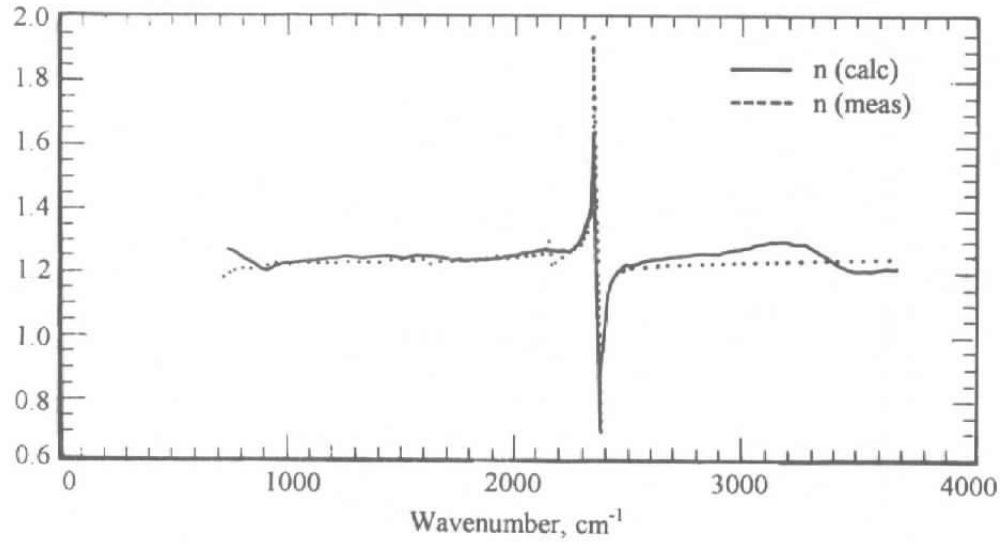

Figure 26. n (calc) and n (meas) of 20K $N_2/H_2O/CO_2/CO$ film.

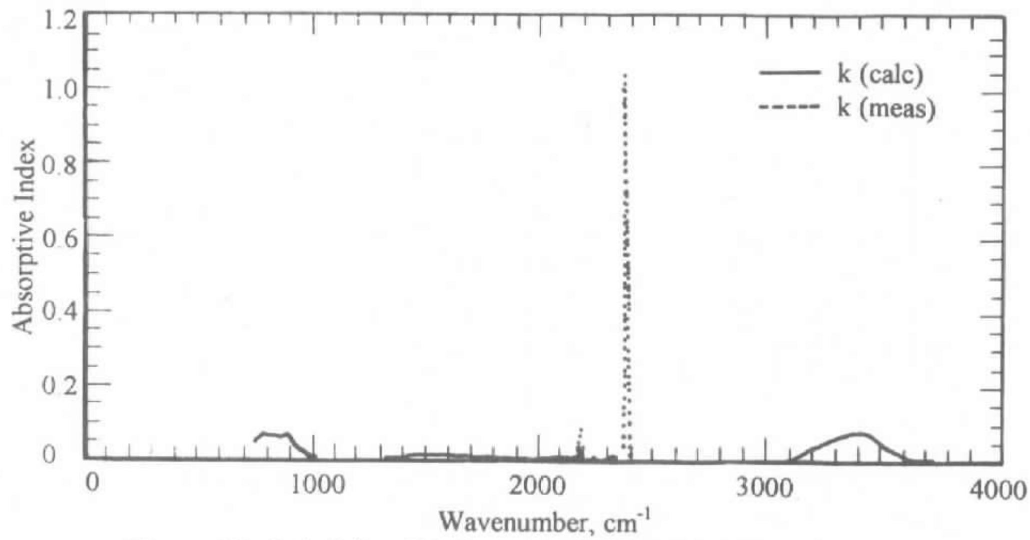

Figure 27. k (calc) and k (meas) of 20K $N_2/H_2O/CO_2/CO$ film.

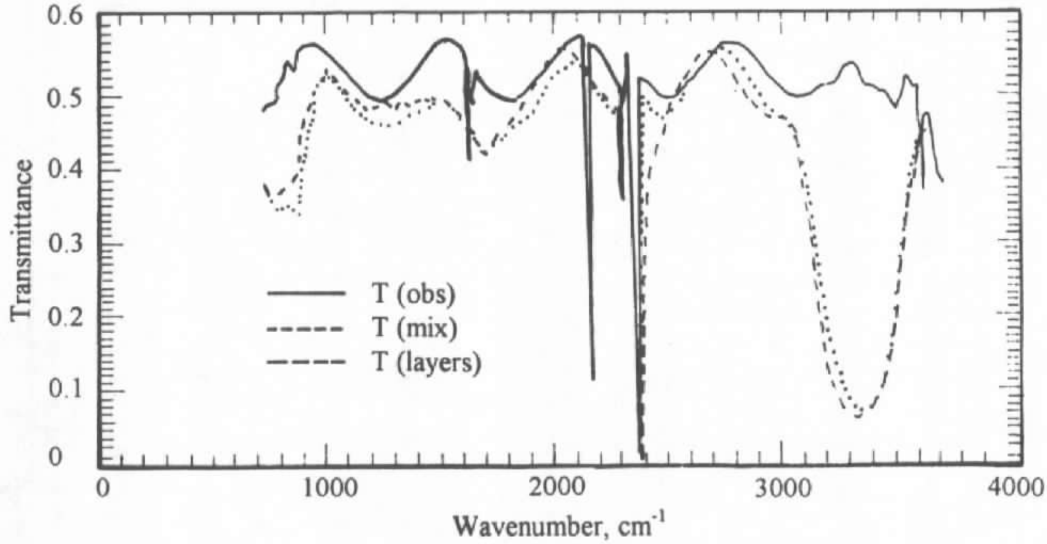

Figure 28. Calculated transmittance of 6.72-µm $N_2/H_2O/CO_2/CO$ film.

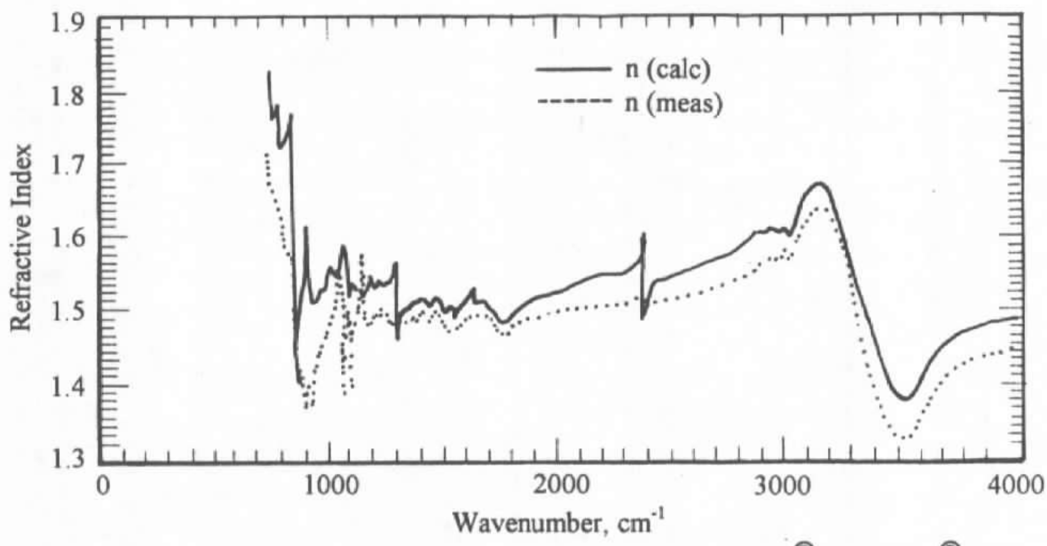

Figure 29. n (calc) and n (meas) of 80K mixture 2 (Uralane® and RTV®) films.

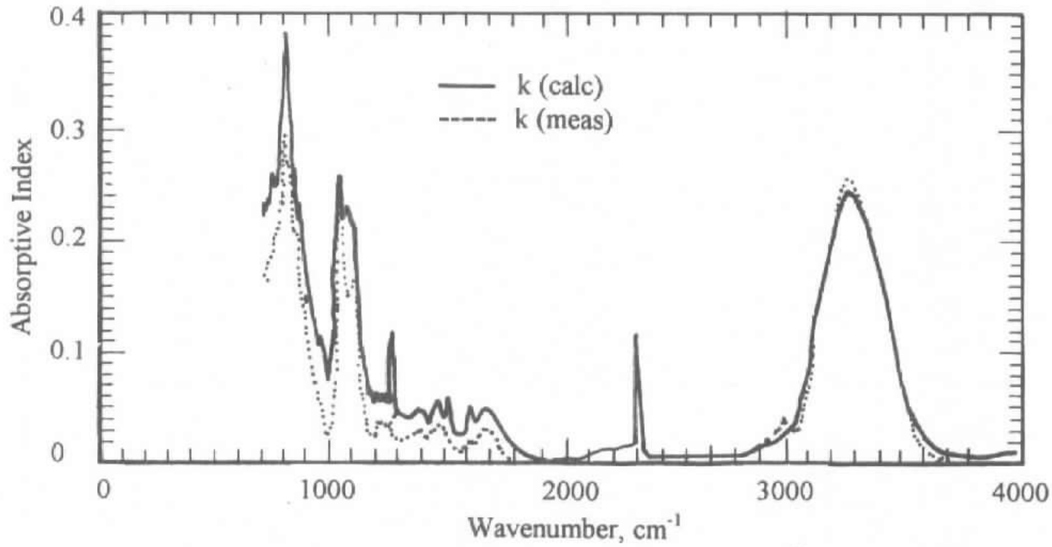

Figure 30. k (calc) and k (meas) of 80K mixture 2 (Uralane® and RTV®) films.

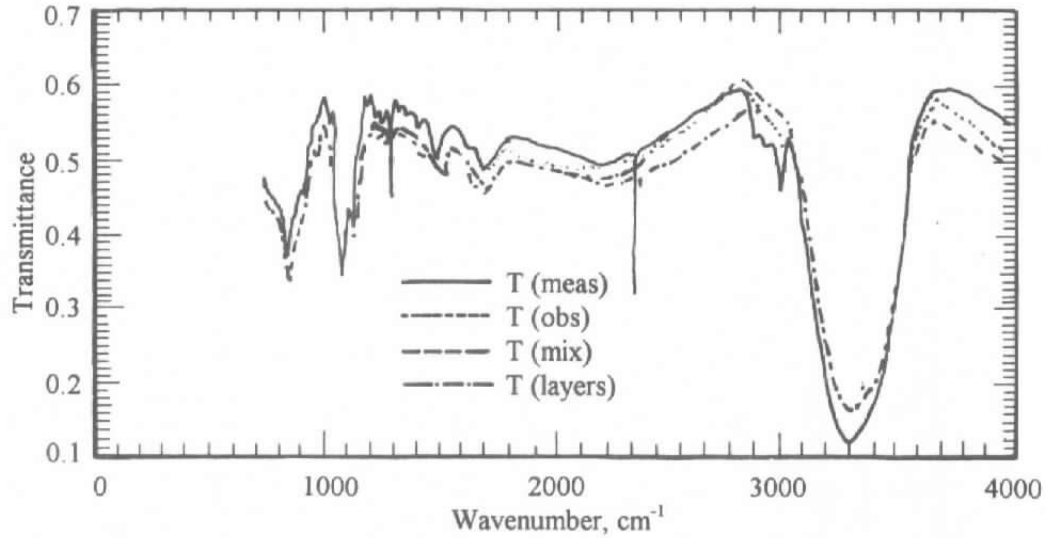

Figure 31. Measured and calculated transmittance of 80K mixture 2 (Uralane® and RTV®) films.

Table 1. Densities of Selected Film Materials

Film	Temperature	Density (kg/m^3)
CO_2	20K	1080
CO_2	80K	1670
H_2O	20K	670
H_2O	80K	920
NH_3	20K	760
NH_3	80K	870
N2	20K	830
CO	20K	800
Uralane®	80K	863
RTV®-566	80K	754
CO_2/CO	20K	950
N_2/CO/CO_2	20K	941
N_2/H_2O/CO_2/CO	20K	770
Mixture 2	80K	938

APPENDIX A
The Lorentz-Lorenz Relation

This appendix contains an outline of the derivation of the classical Lorentz-Lorenz relation which relates the concentration of molecules of a lih dielectric to its complex refractive index. The discussion is similar to those given by Guenther (Ref. 12) and Born and Wolf (Ref. 13).

Suppose, for the moment, that each molecule in the dielectric has a single charge, q, of mass, μ, which acts as a damped harmonic oscillator to give the optical properties of the dielectric. If x is the displacement of the oscillator from equilibrium and E_{loc} is the component of the local electric field experienced by the oscillator, Newton's Second Law gives the following equation of motion:

$$\ddot{x} + \gamma\dot{x} = \omega_0^2 x = \frac{qE_{loc}}{\mu}, \tag{A-1}$$

where γ and ω_0 are the damping and simple harmonic frequency constants, respectively.

To make the connection between macroscopic and microscopic quantities, one can use the polarization density P = Np, where N is the number density of the oscillators and p = qx is the electric dipole moment per oscillator. The local electric field is related to P and the "cavity" (or measured) value of the electric field E by $E_{loc} = E + aP$ (Eq. (3)). Furthermore, for linear dielectrics, E and P are linearly proportional: $P = \chi E$. These relations allow the equation of motion to be rewritten in terms of P and its time derivatives. If we make the assumption that the incident electric field E has a frequency w and a time dependence of $\exp[-i\omega t]$, the constant c can be found from the equation of motion to be

$$\chi = \frac{\frac{Nq^2}{\mu}}{\omega_0^2 - \omega^2 \frac{Naq^2}{-\mu} - i\gamma\omega}. \tag{A-2}$$

The relationsiop of χ to the complex optical index **n** of a dielectric comes from the "constitutive" relation between the displacement field D and the electric field E, which is $\vec{D} = \varepsilon_0\vec{E} + \vec{P} = \varepsilon\vec{E}$, where ε is the (complex) electric permittivity of free space. This means that $\varepsilon = \varepsilon_0 + \chi$. Because the refractive index **n** for a nonmagnetic dielectric is $\mathbf{n} = (\varepsilon/\varepsilon_0)^{\frac{1}{2}}$, the desired relation between χ and n is

$$\chi = \varepsilon - \varepsilon_0 = \varepsilon_0(\mathbf{n}^2 - 1). \tag{A-3}$$

When one equates Eqs. (A-2) and (A-3) and does some algebraic manipulation, the result is

$$\frac{\mathbf{n}^2 - 1}{\mathbf{n}^2 + b} = \frac{\dfrac{Nq^2}{\varepsilon_0 \mu}}{\omega_0^2 - \omega^2 \dfrac{Naq^2}{-\mu} - i\gamma\omega}, \tag{A-4}$$

where constant b is given by Eq. (4).

Equation (A-4) is one form of the Lorentz-Lorenz relation, but the relation is often given in terms of the mean polarizability which relates the (average) electric dipole moment per molecule, p, with the local electric field E_{loc} in a lih dielectric: $p = \alpha E_{loc}$. If the original equation of motion, Eq. (A-1), is recast in terms of α and the time derivatives of P, α turns out to be

$$\alpha = \frac{\dfrac{q^2}{\mu}}{\omega_0^2 - \omega^2 - i\gamma\omega}. \tag{A-5}$$

The Lorentz-Lorenz formula of Eq. (1) follows when Eq. (A-5) is multiplied by Na and compared to Eq. (A-4).

If each molecule has more than one oscillator, the Lorentz-Lorentz relation of Eq. (1) is still valid because of the linear relationship of the electric dipole moment p and the local electric field E_{loc} (See Ref. 12).

If the dielectric is a homogeneous mixture of non-interacting molecule species, each with a number density N_j *within* the mixture, the mean polarizability of the mixture α is the mathematical weighted mean of the individual polarizabilities for each species α_j, $\alpha = (\Sigma N_j \alpha_j)/N$, where N is the total number density of molecules in the mixture, $N = \Sigma N_j$. A value of α_j can be calculated from Eq. (1) using the value of the complex index $\mathbf{n}_j$ and number density N_{pj} measured for the jth molecular species *in its pure state.* When these relations are combined with the corresponding equation for a of the mixture, α is

$$\alpha = \left(\frac{1}{Na}\right)\left[\frac{\mathbf{n}^2 - 1}{\mathbf{n}^2 + b}\right] = \Sigma\left(\frac{N_j/N}{N_{pj}a_j}\right)\left[\frac{\mathbf{n}_j^2 - 1}{\mathbf{n}_j^2 + b_j}\right], \tag{A-6}$$

where the local field parameters are a_j and $b_j = (\varepsilon_0 a_j)^{-1} - 1$, for the jth component in its pure state, and a and $b = (\varepsilon_0 a)^{-1} - 1$ for the mixture. When one solves Eq. (A-6) for $\mathbf{n}$, Eqs. (8) and (9) result.

APPENDIX B
Transmittance and Reflectance of a Stack of Multilayers in the Case of Phase Coherence Within the Films

Potter (Ref. 6) discusses the transmittance and reflectance of a stack of uniform multilayers on a substrate (Fig. 3) using the (arbitrary) choice of exp[iwt] for the time dependence of an incident light beam. This forces one to define the complex refractive index to be $\mathbf{n}$ = n - ik and makes a difference in some of the other defined quantities and derived equations. This appendix gives the major changes in the article by Potter that result from a field time dependence choice of exp[-iwt] which, among other things, makes $\mathbf{n}$ = n + ik. The stack (in Fig. 3) has N_i uniform films ahead of the substrate (labeled s) and N_b films on the back side of the substrate.

The wave equations of the fields that come from Maxwell's Equations do not change with the choice of time dependence, but the signs of the exponents for the field quantities in the TE and TM modes are reversed as Eqs. (10-14) show when compared to the corresponding equations in Ref. 6. There are sign reversals as well in Eqs. (5a) and (5b) of Ref. 6 for U' and V' and in the off-diagonal terms of the matrix in Eq. (10) of Ref. 6. The transfer matrix S_{jm} (Eq. (15)) is unchanged from Eq. (13a) of Ref. 6, but the exponents of L (Eq. (17)) have their signs reversed from those in Eq. (14) of Potter (Ref. 6).

In the case of interference within the films and substrate, the algorithm in program STACK incorporates Eqs. (26), (27), and supporting equations of Ref. 6; if interference occurs in the films but not the substrate, STACK uses Eqs. (29) and (31) of Ref. 6 (and their supporting equations). There are several corrections, however. The exponentials in Potter's Eq. (30) should be deleted, and, most importantly, $\hat{\tau}'_f$, which appears in Ref. 6 just before Eq. (31), has the definition, $\hat{\tau}'_f = \hat{\tau}'_{fn} \ldots \hat{\tau}'_{f2}\, \hat{\tau}'_{f1}$. Here, $\hat{\tau}'_{fj}$ represents the Fresnel transmittance coefficient at the jth interface for a beam passing from the substrate to the front surface of the stack.

Another important note is that the quantities, ξ_j, appearing in the definition of the transmission and reflection coefficients (Eq. (16)) depend on the polarization mode of the beam. Because only ratios of ξ_j appear in the transmittance and reflectance equations, multiplicative constants common to all of them can be neglected. In the case of nonmagnetic materials, ξ_j is proportional to $1/\gamma_j$ in the perpendicular (TE) mode and proportional to $-\mathbf{n}_j^2/\ \gamma_j$ in the parallel (TM) mode. γ_j can be found from

$$\gamma_j^2 = \mathbf{n}_j^2 - (n_0 \sin\phi_0)^2, \tag{B-1}$$

where n_0 is the (real) refraction index, and ϕ_0 is the beam angle in the incident medium, and $\mathbf{n}_j$ is the complex refraction index of the jth medium.

APPENDIX C
Transmittance and Reflectance of A Stack of Multilayers in the Case of No Phase Coherence Within the Films or Substrate

This appendix outlines an extension of Potter's analysis to the case of a light beam incident on films supported by a substrate in which no interference occurred anywhere in the stack. In this case, the transfer matrices relate beam intensities at various points within the stack instead of beam amplitudes, as in the case of film phase coherence (Figs. 1-3). As above, the stack has N_i uniform films ahead of the substrate (labeled s) and N_b films on the back side of the substrate.

For either polarization (TEM or TMM), the reflectance and transmittance of a beam incident on the stack are, respectively,

$$R = \frac{R_{0s} + R_{sf} D_{0s} E_s^2}{1 + R_{s0} R_{sf} E_s^2}, \tag{C-1}$$

and

$$T = \frac{T_{0s} T_{sf} E_s^2}{1 + R_{s0} R_{sf} E_s^2}. \tag{C-2}$$

R_{0s} and T_{0s} are the reflectance and transmittance, respectively, of a beam going from the non-absorbing incident medium (semi-infinite medium 0) into the substrate, R_{s0} and T_{s0} are the corresponding quantities for a beam originating in the substrate and traveling to the front surface, and R_{sf} and T_{sf} refer to analogous quantities of a beam originating in the substrate and entering the exit medium (semi-infinite medium f). In the jth medium, the exponential decay term E_j is

$$E_j = \exp\ [-2\mathrm{Im}\,(\delta_j)\,], \tag{C-3}$$

where

$$\delta_j = 2\pi\nu\gamma_j\, d_j.$$

γ_j is defined in Eq. (B-1), and d_j is the thickness of the jth medium. Im refers to the imaginary part of a complex number.

D_{0s} and the various transmittances and reflectances in Eqs. (C-1) and (C-2) come from the intensity transfer matrices for the stack. These matrices are themselves products of the intensity matrices at an interface and through a uniform medium defined in Eqs. (18-20). The total transfer matrix M for the stack is analogous to the one Potter gives for films supported by a substrate and is

found from,

$$\begin{bmatrix} I_0^+ \\ I_0^- \end{bmatrix} = M \begin{bmatrix} I_f^+ \\ 0 \end{bmatrix}, \tag{C-4}$$

where

$$M = M_{0s} M_s M_{sf}.$$

M_{0s} is the intensity transfer matrix for the beam going from the incident medium into the substrate and is a product of the matrices in Eqs. (18) and (20) appropriate to the media,

$$M_{0s}\zeta = \Xi_{01}\zeta_1\Xi_{12}\zeta_2 \ldots \Xi_{N_i-1,N_i}\zeta_{N_i}\Xi_{N_i,s}$$

$$= \frac{1}{\Im_{0s}} \begin{bmatrix} a_{0s} & b_{0s} \\ c_{0s} & d_{0s} \end{bmatrix} \tag{C-5}$$

$$= \frac{1}{T_{0s}} \begin{bmatrix} 1 & R_{s0} \\ R_{0s} & D_{0s} \end{bmatrix},$$

where

$$\Im_{0s} = T_{01} T_{12} \ldots T_{Ni,s}. \tag{C-6}$$

T_{jm} comes from Eq. (19), $T_{0s} = \Im_{0s}/a_{0s}$, $R_{0s} = c_{0s}/a_{0s}$, $R_{s0} = b_{0s}/a_{0s}$ and D_{0s}/a_{0s}. Similarly, M_{sf} represents the intensity transfer matrix for a beam going from the substrate to the exit medium and is

$$M_{0s} = \Xi_{s,s+1}\zeta_{s+1}\Xi_{s+1,s+2}\zeta_{s+2} \ldots \Xi_{s+N_b-1,s+N_b}\Xi_{s+N_b f} \tag{C-7}$$

$$= \frac{1}{\Im_{sf}} \begin{bmatrix} a_{sf} & b_{sf} \\ c_{sf} & d_{sf} \end{bmatrix}$$

$$= \frac{1}{T_{sf}} \begin{bmatrix} 1 & R_{sf} \\ R_{sf} & D_{sf} \end{bmatrix},$$

where

$$\Im_{sf} = T_{s,s+1} T_{s+1,s+2} \cdots T_{s+Nb,f}, \tag{C-8}$$

$T_{sf} = \Im_{sf}/a_{sf}$, $R_{sf} = c_{sf}/a_{sf}$, $R_{fs} = b_{sf}/a_{sf}$, and D_{sf}/a_{sf}. The intensity matrix M_s through the substrate is

$$M_s = \zeta_s. \tag{C-9}$$

Program STACK uses the relations in Eqs. (C-1 through C-9) to compute the transmittance and reflectance of a light beam for the case that no interference occurs in the films or substrate.

APPENDIX D
Complex Arithmetic in TBL

This note is to caution users of Version 3.1 of the Interactive Data Language (IDL (tm)) for Windows, from research Systesm, Inc. of Boulder, Colorado, that serious computational errors may occur when one sues IDL to compute the square roots of complex numbers. In IDL, the real and imaginary parts of a complex number are single precision ("FLOATING"). If one uses the SQRT function to find the square root of a complex number whose imaginary part is small compared to its real part (or vice-versa), the imaginary (or real) part of the square root may be in serious error.

In one test, IDL program CMPLXTST, the real part of a complex number z is fixed at one and the imaginary part decreases from one by successive division by 10. The program compares z with the supposedly equivalent SQRT(z^2). Though only small roundoff errors occur for imaginary values greater than or equal to 10^{-3}, for imaginary part values of z of 10^{-4} or less, the imaginary part of SQRT(z^2) is zero.

To remedy this situation, one may compute the square root of any complex number by finding, in double precision, the modulus and angle of its polar form in the complex plane and then multiplying the square root of the modulus by the sum of the cosine of half of the angle of z and i times the sin of the same half angle. In fact, before this correction was applied to one of the AEDC programs, the result of a certain calculation involving a complex square root was 1.0 instead of the expected value of about 0.3.